KTH Electrical Engineering

Measurement Techniques for Characterization of Power Amplifiers

DAVID WISELL

Doctoral Thesis in Telecommunications
Stockholm, Sweden 2007

2

Abstract

In this thesis a sampling time domain measurement system primarily intended for measurements on radio frequency power amplifiers is discussed. The need for such a measurement system is established. Impairments due to non-ideal measurement instruments are discussed as well as methods to compensate for these impairments. Techniques to improve upon the raw measurement performance of the measurement instruments with regard to bandwidth, dynamic range, linear and nonlinear distortion are discussed.

A method to simultaneously find the phase and amplitude ripple of a vector signal generator and a vector signal analyzer is presented. The method is verified with extensive measurements.

Two techniques, frequency stitching and Zhu's generalized sampling theorem, to extend the effective measurement bandwidth of the measurement system is discussed and evaluated with measurements. They are both found to be able to extend the effective bandwidth for measurements of output signals of nonlinear power amplifiers with more than five times.

The measurement system is used for sampled input – output measurements of power amplifiers and the obtained data are fitted to different behavioral power amplifier models including memory. Some different behavioral models are evaluated and compared for different kinds of power amplifiers. A neural network model and extensions to the well-known parallel Hammerstein model are specifically discussed. The parallel Hammerstein model are also used together with frequency stitching and Zhu's generalized sampling theorem.

A general hardware and software structure of a versatile measurement system based on virtual instruments for measurements on power amplifiers is discussed in some detail. Special attention is given to the software architecture and to the concepts of hardware and software reusability.

An automated, fast, accurate and production-friendly method for two-tone power and frequency sweep measurements, including measurement of the phase of the intermodulation products in addition to the amplitude, is also presented.

Acknowledgment

David Wisell
Söderfors, October 2007

Contents

1 Introduction

1.1 Background

Measurement technology for radio frequencies (RFs) has underwent, and is still undergoing, a rapid technology shift from analog to digital techniques, similar to what has previously happened to wireless communication technology.

The shift from analog to digital has had profound consequences for the design, modeling and characterization of critical radio components such as the power amplifier (PA), a key component of radio basestations (RBSs) [1]. The PA must now be designed to possibly handle digital modulated signals with bandwidths of tenths of MHz and a fast changing envelope with a considerable peak-to-average power ratio (PAPR). Such signals are a far distance from narrow-banded constant envelope signals of earlier systems such as GSM. There is also a trend toward higher and higher efficiency requirements on the PA. This has led to a plethora of techniques that tries to meet these requirements [2], [3]. A natural consequence is the increased need for measurement methods and techniques tailored to meet the requirements for these applications. The measurement technology becomes a key enabler both for design, verification or production testing of these PAs. Typically sampled measurement systems are used, i.e. the output signal, and sometimes also the input signal, of the PA are downconverted and sampled [4], [5] and [6]. The sought information, for design, verification or production testing purposes, is then extracted using digital signal processing (DSP).

Further, more and different information about the PAs are often needed when they are integrated with DSP algorithms, e.g. digital predistortion (DPD), in order to increase their performance with regard to linearity and efficiency. This is probably also true for most of the emerging PA technologies.

Measurement methods based on downconversion and sampling of the RF signals, as well as behavioral or black-box modeling of the PA, often focus on the first spectral zone around the RF carrier. This is also the focus of the measurement methods and techniques developed in this thesis.

The measurement requirements for PA characterization can often not be fully met using commercial off-the-shelf (COTS) instrumentation. Instead different techniques to increase the raw instrument performance have to be applied. The most critical parameters are often the bandwidth and dynamic range of the measurement system.

The main focus of this thesis is the development of methods to increase the performance of a measurement system for measurements of radio components beyond the raw performance of the measurement instruments. Most of the techniques that have been developed in this thesis have originally had PA measurements in mind, but are equally useful for measurements on other

components or entire transmitters as well. This is important since the PA technology is developing towards integrated solutions with digital input and RF output signals [1] and the term transmitter, rather than PA, architecture, may be more appropriate [2].

Finally some PA models are developed and discussed based on the measurements taken using the developed measurement system.

This thesis is basically built on the publications listed in Ch. 1.2 which are appended. The remaining publications produced during the course of the work are listed in Ch. 1.3.

The outline is as follows. In Ch. 2 traditional techniques for nonlinear characterization of PAs are briefly treated. A motivation to complement the techniques in Ch. 2 with methods aimed at wideband digitally modulated signals is given in Ch. 3. A measurement system for measurements on such signals is introduced in Ch. 4. In Ch. 5 the performance of this measurement system is enhanced through various techniques built on DSP. In Ch. 6 the measurement system is put to work for the purpose of PA model identification and development. In Ch. 7 a short summary of the papers in Ch. 1.2 is given.

1.2 Contributions

This thesis builds on the work presented in the following publications. The publications considered most significant for *this* thesis are labeled [Paper A-L] and appended in the end of the thesis. They are introduced and referenced as [Paper A-L] throughout the text, while some of the others are listed in Ch. 1.3 and referenced in the reference list. The contribution to each paper, [Paper A]-[Paper L], is stated in Ch. 7.

[Paper A]   M. Isaksson, D. Wisell, and D. Rönnow, "Wideband Dynamic Modeling of Power Amplifiers Using Radial-Basis Function Neural Networks," *IEEE Trans. Microwave Theory Tech.*, vol. 53, pp. 3422-28, 2005.

[Paper B]   M. Isaksson, D. Wisell, and D. Rönnow, "A Comparative Analysis of Behavioral Models for RF Power Amplifiers," *IEEE Trans. Microwave Theory Tech.*, vol. 54, pp. 348-359, 2006.

[Paper C]   D. Rönnow, D. Wisell, and M. Isaksson, "Three-Tone Characterization of Nonlinear Memory Effects in Radio Frequency Power Amplifier." *To appear, IEEE Trans. Instrum. Meas.*

[Paper D]   D. Wisell, B. Rudlund, and D. Rönnow, "Characterization of Memory Effects in RF Power Amplifiers Using Digital Two-Tone

10

Measurements," *To appear, IEEE Trans. Instrum. Meas.*

[Paper E] D. Wisell, D. Rönnow, and P. Händel, "A Technique to Extend the Bandwidth of a Power Amplifier Test-bed," *IEEE Trans. Instrum. Meas.*, vol. 56, pp. 1488-1494, 2007.

[Paper F] D. Wisell and P. Händel, "Simultaneous Measurement of Transmitter and Receiver Magnitude and Phase Ripple," *Submitted to Measurement Jan 2007.*

[Paper G] D. Wisell, "A Baseband Time Domain Measurement System for Dynamic Characterisation of Power Amplifiers with High Dynamic Range over Large Bandwidths," presented at IEEE Instrum. Meas. Tech. Conf., Vail, Colorado, 2003, pp. 1177-80.

[Paper H] D. Wisell, M. Isaksson, N. Keskitalo, and D. Rönnow, "Wideband Characterization of a Doherty Amplifier Using Behavioral Modeling," presented at ARFTG 67, San Fransisco, 2006, pp. 190-99.

[Paper I] D. Wisell, "Exploring the Sample Rate Limitation for Modeling of Power Amplifiers," presented at IMEKO 2006, Rio de Janeiro, 2006.

[Paper J] D. Wisell and N. Keskitalo, "A Behavioral Power Amplifier Model that Includes the Average Power Level," presented at ARFTG 68, Boulder, CO, 2006.

[Paper K] D. Wisell and P. Händel, "Implementation Considerations on the Use of Zhu's General Sampling Theorem for Characterization of Power Amplifiers," presented at IEEE Instrum. Meas. Tech. Conf., Warzaw, 2007.

[Paper L] D. Wisell, P. Stenvard, A. Hansebacke and N. Keskitalo, "Considerations when Designing and Using Virtual Instruments as Building Blocks in Flexible Measurement System Solutions," presented at IEEE Instrum. Meas. Tech. Conf., Warzaw, 2007.

1.3 Other Publications

These publications have also been produced during the course of the work but are not appended to the thesis, but some are referenced in the text.

D. Wisell and T. Öberg, "Effects of Non-Linear Distortion on Adjacent Channel Interference in WCDMA Systems," presented at RVK 99, Karlskrona, Sweden, 1999, pp. 668-72.

D. Wisell and T. Öberg, "Analysis and Identification of Transmitter Non-

linearities," presented at CSNDSP2000, Bournemouth, England, 2000, pp. 418-21.

D. Wisell, "Identification and Measurement of Transmitter Non-Linearities," presented at ARFTG 56 2000, Boulder, USA, 2000, pp. 104-109.

O. Andersen, P. Malmlöf, and D. Wisell, "Nonlinear Characterization of Multiple Carrier Power Amplifiers," presented at ARFTG 56 2000, Boulder, USA, 2000, pp. 151-58.

D. Wisell, "A Baseband Time Domain Measurement System for Dynamic Characterisation of Power Amplifiers with High Dynamic Range over Large Bandwidth," Licentiate Thesis, Uppsala University, Uppsala, Sweden, 2004.

M. Isaksson and D. Wisell, "Extension of the Hammerstein Model for Power Amplifier Applications," presented at ARFTG 63, Fort Worth, USA, 2004, pp. 131-37.

M. Isaksson, D. Wisell, and D. Rönnow, "Nonlinear Behavioral Modeling of Power Amplifiers Using Radial-Basis Function Neural Networks," presented at IEEE MTT-S, Los Angeles, 2005, pp. 1967-70.

D. Wisell, M. Isaksson, and D. Rönnow, "Validation of Behavioural Power Amplifier Models Using Coherent Averaging," presented at Gigahertz 2005, Uppsala, Sweden, 2005, pp. 318-21.

M. Isaksson, D. Wisell, and D. Rönnow, "Behavioural Amplifier Modelling Using Sampled Complex Envelope Measurement Data," presented at Gigahertz 2005, Uppsala, Sweden, 2005, pp. 213-16.

D. Wisell, "A Step Towards a More General Behavioral Power Amplifier Model," presented at Power Amplifier Workshop 2006, San Diego, USA, 2006.

D. Wisell, D. Rönnow, and P. Händel, "A Bandwidth Extension Technique for Dynamic Characterization of Power Amplifiers," presented at IEEE Instrum. Meas. Tech. Conf. 2006, Sorrento, Italy, 2006, pp. 1972-76.

D. Wisell, M. Isaksson and N. Keskitalo, "A General Evaluation Criteria for Behavioral Power Amplifier Modeling," presented at ARFTG 69, Honolulu, USA, 2007, pp. 251-55.

M. Isaksson, D. Wisell, A. Eng and D. Rönnow, "A Study of a Variable-Capacitance Drain Network's Influence on Dynamic Behavioral Modeling of an RF Power Amplifier," presented at ARFTG 69, Honolulu, USA, 2007, pp. 112-16.

D. Wisell, M. Isaksson, "Derivation of a Behavioral RF Power Amplifier Model with Low Normalized Mean-Square Error", presented at European Microwave Conf., Munich, Germany, 2007.

O. Andersen, N. Keskitalo, P. Stenvard and D. Wisell, "Cost Effective High Performance Modular Instrumentation, Signal Generation and Signal Analysis for Future Mobile Communication Systems,", presented at Autotestcon 2007,

12

Baltimore, USA, 2007, pp. 660-68.

D. Wisell, P. Stenvard, A. Hansebacke and Niclas Keskitalo, "Considerations when Designing Virtual Instruments", *Submitted to IEEE Trans. Instrum. Meas. June 2007.*

1.4 Abbreviations

ACEPR	Adjacent Channel Error Power Ratio
ACLR	Adjacent Channel Leakage Ratio
ADC	Analog-to-Digital Converter
AM/AM	Amplitude Dependent Amplitude Distortion
AM/PM	Amplitude Dependent Phase Distortion
ASIC	Application Specific Integrated Circuit
COTS	Commercial off-the-shelf
CW	Continues Wave, i.e. sinusoidal signal
DAC	Digital-to-Analog Converter
DPA	Driver Power Amplifier
DPD	Digital Predistortion
DSO	Digital Sampling Oscilloscope
DSP	Digital Signal Processing
DUT	Device Under Test
EER	Envelope Elimination and Restoration
ET	Envelope Tracking
FPGA	Field Programmable Gate Array
IF	Intermediate Frequency
IM	Intermodulation
IM3	Third-Order Intermodulation
IP3	Third-Order Intercept Point
LDMOS	Laterally Diffused Metal Oxide Semiconductor
LO	Local Oscillator
LPF	Low Pass Filter

LSNA	Large Signal Network Analyzer
MER	Memory Effect Ratio
NMSE	Normalized Mean-Square Error
NVNA	Nonlinear Vector Network Analyzer
OFDM	Orthogonal Frequency Division Multiplexing
PA	Power Amplifier
PAPR	Peak-to-Average Power Ratio
RBS	Radio Basestation
RBW	Resolution Bandwidth Filter
RF	Radio Frequency
SDM	Software Driven Measurements
SI	Synthetic Instrument
TDFT	Time-Discrete Fourier Transform
VI	Virtual Instrument
VSA	Vector Signal Analyzer
VSG	Vector Signal Generator
WCDMA	Wideband Code Division Multiple Access
ZGST	Zhu's Generalized Sampling Theorem

1.5 Notations

These notations are used throughout this thesis. Other notations are used in the papers in the Appendix.

$a(t)$, $a(n)$	Amplitude modulation
ε	Model error
$\varepsilon(t)$	Error signal
$e(n)$	Error signal
$E(f)$	TDFT of $e(n)$

14

$H(q^{-1})$	Discrete-time linear filter
$I(n)$	In-phase signal
j	$\sqrt{-1}$
$K(\cdot)$	General nonlinear function with memory
M	Constant that sets the number of filter coefficients
n	Discrete time
ω_c	Angular carrier RF
$\varphi(t)$, $\varphi(n)$	Phase modulation
$p(n)$	Power envelope
P	Constant that sets the nonlinear order
$Q(n)$	Quadrature-phase signal
$s(t)$	Modulated RF signal
$\tilde{s}(t)$	Hilbert transform of $s(t)$
t	Continues time
$u(n)$	Input signal to the PA on complex envelope form
$U(f)$	TDFT of $u(n)$
$y(n)$	Output signal from the PA on complex envelope form
$y_{meas}(n)$	Measured output signal from the PA on complex envelope form
$y_{sim}(n)$	Output signal from the PA model on complex envelope form
$y'(n)$	The $y(n)$ time-aligned to $u(n)$
$Y_{meas}(f)$	TDFT of $y_{meas}(n)$
$Y_{sim}(f)$	TDFT of $y_{sim}(n)$

16

2 Traditional Techniques for Characterization of Power Amplifiers

Power amplifiers have traditionally been characterized with respect to linearity using power swept continues wave (CW) signals to find the AM/AM and AM/PM distortion and the 1 dB compression point, or simple two-tone measurements to find the third-order intercept point (IP3). The AM/AM distortion is the amplitude distortion as a function of the amplitude of an input CW signal and AM/PM is the phase distortion as a function of the same amplitude. Typical AM/AM and AM/PM traces are shown in Fig. 1 and Fig. 2, respectively. The measurement is taken at one frequency at a time and there is a strict one-to-one relationship between the input power and the AM/AM and AM/PM.
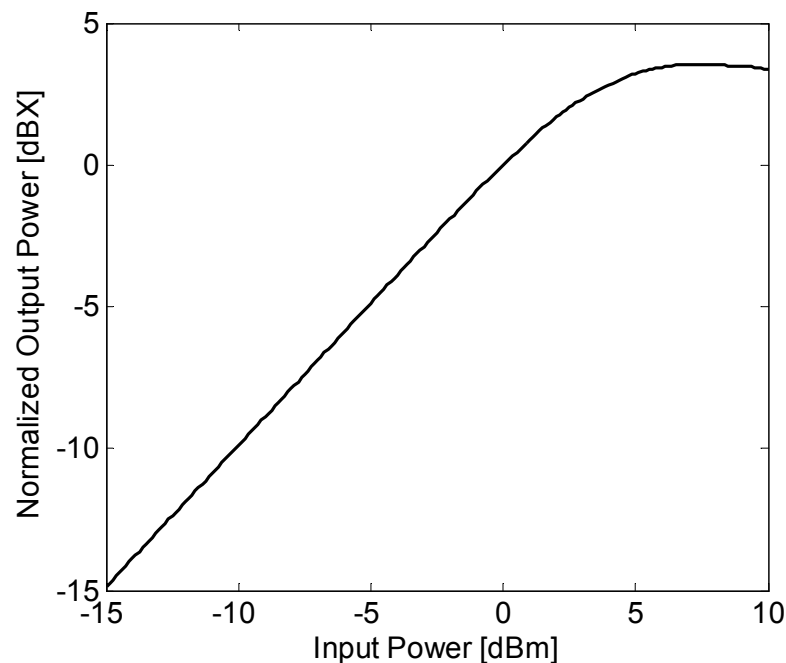
Fig. 1. AM/AM distortion. The output power as a function of the input power. Measured with a power swept CW signal at a certain frequency using a vector network analyzer.
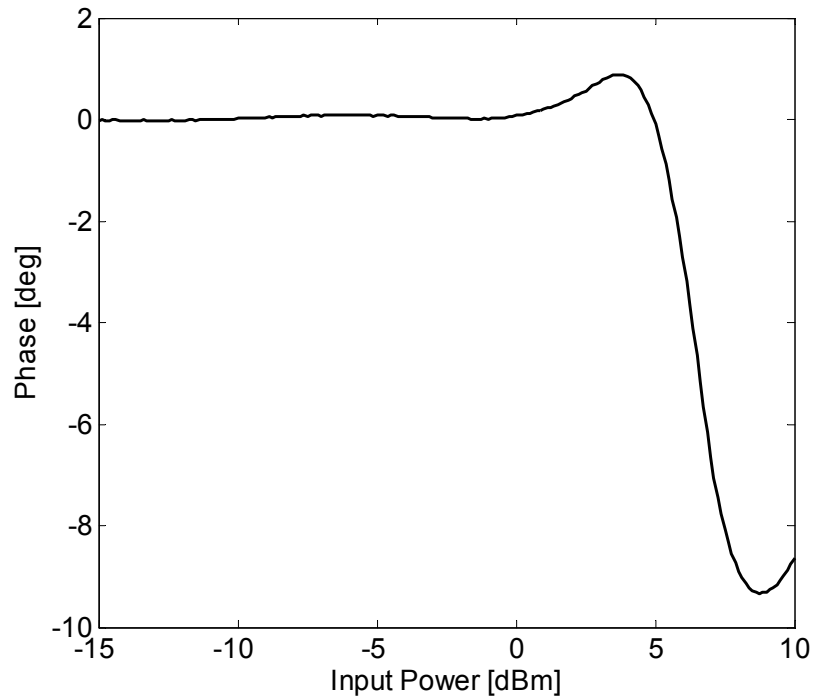
Fig. 2. AM/PM distortion. The phase distortion in the output signal as a function of the input power. Measured with a power swept CW signal using a vector network analyzer.

The 1 dB compression point is the power level at which the gain is one dB lower than the small signal gain. The third-order intercept point is illustrated in

Fig. 3. It is the point at which the third-order intermodulation products (IM3) in a two-tone test equals the fundamental. This point is obtained by extrapolating measurements of the IM3 and the fundamentals done at lower input power levels. The fundamental has a 1:1 slope and the IM3 has a 1:3 slope, i.e. if the input power is increased 1 dB the IM3 increase 3 dB. The IP3 can be related to either the input or output power level. For amplifiers it is normally referenced to the output power level.

While these measurements are still valid and important, they fail in some respects to give information about the amplifier that is needed when implementing several of the linearization and efficiency enhancement techniques that are now widely used see e.g. [1] and [3]. Neither do the traditional measurements give enough information to design highly accurate models of the PAs, as described below.

18

Output Power (dBm)
Input

Fundamentals

IP3

1:1

Actual behavior
of the amplifier

1:3

IM3
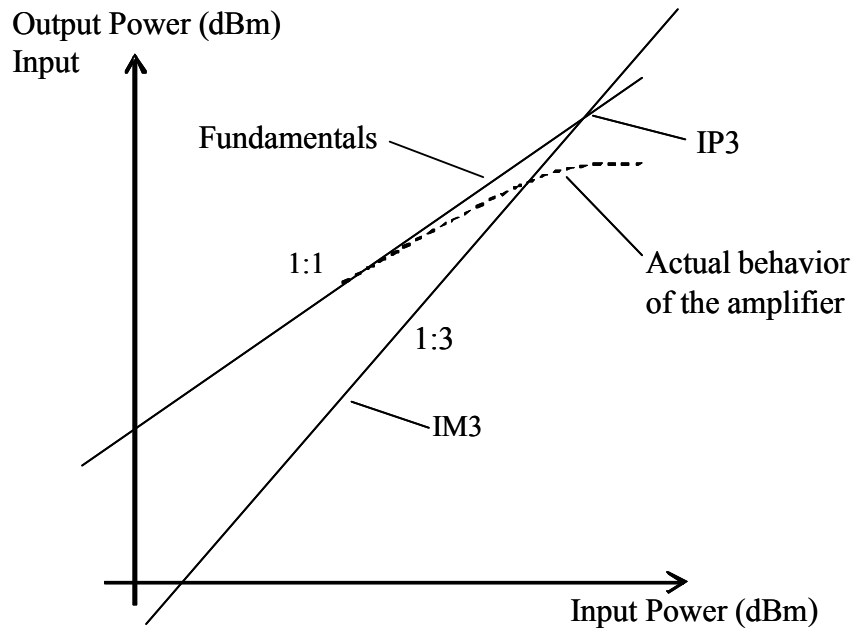
Input Power (dBm)

Fig. 3. Third-order intercept point. The IP3 is the point at which the amplitude of the two fundamentals and the IM3 would be equal if the two fundamentals increase with a 1:1 slope and the IM3 increases with a 1:3 slope as functions of the input power until they meet.

As already mentioned, power swept CW measurements have traditionally been used for nonlinear characterization of PAs. It is now well-known that such measurements will not reveal the actual behavior of the amplifier when subject to a digitally modulated signal having a large PAPR, a fast changing envelope and a bandwidth of several MHz. This was noted by Bösch in 1989 [7]. In [8] a two-tone measurement with different tone separation and recording of the AM/AM and AM/PM distortion was done. The results in both [7] and [8] indicated that the traditional nonlinear narrow band measurements were not capable of predicting the behavior of PAs when subjected to advanced digitally modulated signals.

One method that was proposed to circumvent the limitations of the two-tone test for nonlinear characterization of PAs was two-tone sweeps in frequency and amplitude. Some examples of this are [3], [9], [10], [11], [12] and [13]. The two-tone sweep in frequency is an extension of the two-tone sweep in power that has been used for years. By sweeping in both frequency and power, a matrix of the intermodulation level for both the upper and lower IM3 are obtained. From this matrix the properties of the amplifier are then derived. Typical such plots are given in e.g. [14], [15] and [16]. Normally only the amplitude of the third, and sometimes fifth, order intermodulation is recorded. When the phase is measured complicated measurement set-ups have been used. Results in the order of a measurement

19

time in hours [13] and a measurement accuracy of a few tenths of a dB and a few degrees are reported from these. See [12] for a comparison on the accuracy that is obtained for different techniques to measure the IM products of two-tone measurements.

In [Paper D] an alternative method to the ones discussed above for measurements of the amplitude and phase of the IM products generated in two-tone testing was discussed. This method makes use of DSP in order to accelerate the measurement speed considerably. The advantages of the proposed technique are, in addition to the measurement speed, the high accuracy, that it will take advantage of new improvements in ADC and DAC technology and that it can be implemented on the same hardware (HW) as the measurement system presented in Ch. 4 and thus integrated into that measurement system.

A technique that is somewhat related to the one explained in [Paper D] but makes use of three, rather that two, tones, in order to find the third-order Volterra Kernels [17] was developed in [Paper C]. Measurement of Volterra kernels have previously been presented in e.g. [18]. The rationale for the three-tone measurements over the two-tone is that it allows complete determination of the third-order Volterra kernel.

Even if numerous attempts, see e.g. [19], [20], [21] and [22] have been made to correlate two-tone measurements to modulation quality parameters, e.g. adjacent channel leakage ratio (ACLR) [23], many applications such as PA modeling and DPD of PAs benefit from the use of more application-like signals, i.e. multitone or modulated signals, in practice. Such techniques are discussed in Ch. 3.

3 Characterization of Power Amplifiers Using Wideband Digitally Modulated Signals

With the introduction of digitally modulated signals with a wider bandwidth and a fast changing envelope, e.g. WCDMA, the requirements on the PA changed. Specifically, the concept of "memory effects" in the PA become of large interest. The origins of such phenomena in the PAs are beyond the scope of this thesis but are explained in [24]. Early PAs for digitally modulated wideband signals did often use the feedforward technology [25] for linearization, partly because it, as a technology, is resistant to the "memory effects". One drawback with the feedforward technology was however the high complexity (read costs), which called for other solutions. This lead to the development of the DPD technique which either requires a "memory less" PA or an advanced DPD that incorporates compensation for the "memory effects". The first solution being a PA design problem and the second being a system identification and compensation problem. The basic concept of DPD is straightforward enough. It is simply to create in inverse model of the PA which is then implemented using signal processing and applied to the signal before it is sent to the PA. Somewhat more detailed descriptions can be found in [1], [2] and [3].

Early measurement systems for characterization of these "memory effects", or nonlinear frequency dependence, were, as mentioned above, based on two-tone sweeps and the like. Sampled systems started to appear in the mid nineties [8] and have become the method of choice for most industry and academic researchers for these kind of measurements, see e.g. [4], [5] and [8]. These measurement systems closely resembles the transmitter architecture in DPD based transmitters [1], [26] and thus may have some applicability also in such applications. The development, calibration and optimization of a measurement system of this kind are the main focus of this thesis and are treated in Ch. 5 (improvement of the performance of this measurement system).

In work previously presented in [6] measurements were taken using a CW and two eight-tone signals with bandwidths of 100 kHz and 1 MHz respectively, see Fig. 4. It is clear that the CW measurement is not valid for the eight-tone signals. When subjected to an eight-tone signal this amplifier will start to show distortion at significantly lower input power levels than what is indicated by the CW measurement. This result clearly attracted some interest at the time since the results in [6] have been used by some instrument manufacturers when advertising commercial software for this kind of measurements, see [27] (Agilent) and [28] (Rohde & Schwarz).

AM/PM Distortion for a 0.8-2.2 GHz 8W Class A GaAs FET Amplifier
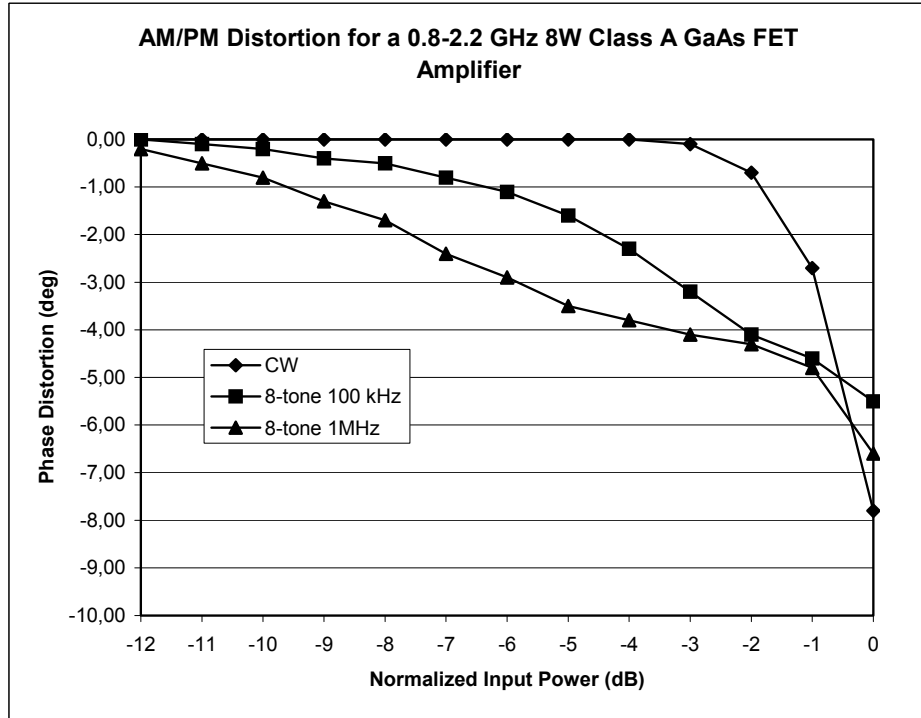
Fig. 4. AM/PM distortion measured using a CW signal and two eight-tone signals with different bandwidth, 100 kHz and 1 MHz. From [6].

The PA technology for cellular RBSs is currently undergoing a rapid development, mainly aimed to increase the efficiency of the PA [1]. Numerous different technologies such as Doherty, Chireix, envelope elimination and restoration (EER), envelope tracking (ET), class-D, E, F, etc PAs and/or combinations of these compete [2]. It is far beyond the scope of this thesis to even briefly touch upon any of these techniques but their introduction will not fundamentally change the need for RF measurement technology? But rather increase it? One difference, however, will be that there will be no measurable RF input signal in the traditional sense for several of these PA techniques of the future.

The measurement technology for PAs will have to evolve with the technology which it is aimed for. Some ideas of what the future might bring for RF measurement systems are treated in Ch. 4.3.

Other techniques than the one discussed in this thesis for characterization of PAs under large signal excitation have been proposed for, loosely speaking, the same purpose. The most known are probably the large signal network analyzer (LSNA), [29], [30], [31], which also goes under numerous other names, e.g. nonlinear vector network analyzer (NVNA).

The LSNA makes use of a technique based on multitones that are applied to a PA driven into its nonlinear regime using one large CW signal. This technique is very

22

different from the PA characterization techniques developed and discussed in this thesis and a comparison of the extracted models using the different techniques in practical applications would be most interesting.

24

4 The Measurement System

This Chapter gives an overview of the measurement system for characterization of PAs that have been developed. A schematic view of the system is shown in Fig. 5. It shall however be remembered that most of what is said here is also true for measurements on other RF components and on entire transmitters.

Similar systems have been proposed elsewhere see e.g., [4], [5], [6] and [8]. With regard to hardware, these differ primarily in how they obtain the input signal of the PA, se below. An alternative, but still somewhat similar, technique treated in e.g. [3], would be to sample the RF input and output signals using a digital sampling oscilloscope (DSO).

The different trade-offs that have to be done when designing measurement systems of the kind in Fig. 5 are discussed in [Paper G] and [32]. hardware limitations and impairments in the measurement system, as well as techniques to overcome them, are treated in Ch. 5.

A more general discussion on hardware and software architecture for measurements system of this kind is also included [Paper L].

4.1 Measurement Signals

The measurement signals that have been used throughout this work can be written as (neglecting noise)

$$s(t) = a(t)\cos(\omega_c t + \varphi(t)) + \varepsilon(t) , \tag{1}$$

where $s(t)$ is the RF measurement signal, $a(t)$ and $\varphi(t)$ the amplitude and phase modulation, respectively, ω_c is the angular frequency of the RF carrier and $\varepsilon(t)$ is all signal content that does not fall in the first spectral zone around ω_c, e.g. harmonics generated by a nonlinear PA.

For the purposes of RF measurement technology development and behavioral PA modeling, the signals can be expressed on complex envelope form. The complex envelope $\tilde{s}(n)$ of (1) in the first spectral zone, i.e. excluding $\varepsilon(t)$ by bandpass filtering around ω_c, after sampling, is

$$\tilde{s}(n) = a(n)e^{j\varphi(n)} = I(n) + jQ(n) , \tag{2}$$

where $I(n)$ and $Q(n)$ are the in-phase and quadrature-phase signals respectively, $j = \sqrt{-1}$ and n is discrete time.

This is the form that will be used in most of the sequel to express the measurement signals.

4.2 The Implemented Measurement System

The measurement system essentially consists of a vector signal generator (VSG) and a vector signal analyzer (VSA), see Fig. 5. The test signal is generated in the PC and downloaded to the VSG that produces the desired modulated signal at the desired RF. This signal might be further amplified using a driver power amplifier (DPA). The output signal of the PA is measured and compared to a reference (input) signal. The reference signal has been chosen somewhat differently by different authors in similar previously published measurement set-ups. In [6] and [8] only the output of the amplifier was measured and the internal digital signal in the VSG was used as reference. In [4], the input and output signals were measured using a VSA with two receivers. In most measurements presented in this thesis the input and output signals have been measured using one receiver, i.e. one VSA. This has the benefit that linear distortion in the VSA cancels, to some degree, between the measurements of the input and output signals, respectively, as described in Ch. 5.3. A requirement for using only one VSA is obviously that a repetitive test signal is used.

The VSA down-converts and samples the signals and returns them to the PC on complex envelope form. Finally the down-converted and sampled input $u(n)$ and output $y(n)$ signals of the PA are time-aligned. The time-alignment is a two-step procedure that involves both time- and frequency domain techniques as first indicated in [Paper G] and further described in [Paper B] and [Paper E]. Here $u(n)$ is used as reference for the time-alignment. The time-aligned version of $y(n)$ is denoted $y'(n)$. An investigation of the properties of the abovementioned time-alignment procedure can be found in [33].

The instruments used for the measurements in this thesis are as VSG, the SMU 200A [34], and as VSA, the FSQ [35]. They are both from Rohde & Schwarz GmbH and shall be considered state-of-the-art in their respective field.

ADC	Analog-to-Digital Converter
DAC	Digital-to-Analog Converter
DPA	Driver Power Amplifier
PA	Power Amplifier
SDM	SW Driven Measurements
VSA	Vector Signal Analyzer
VSG	Vector Signal Generator
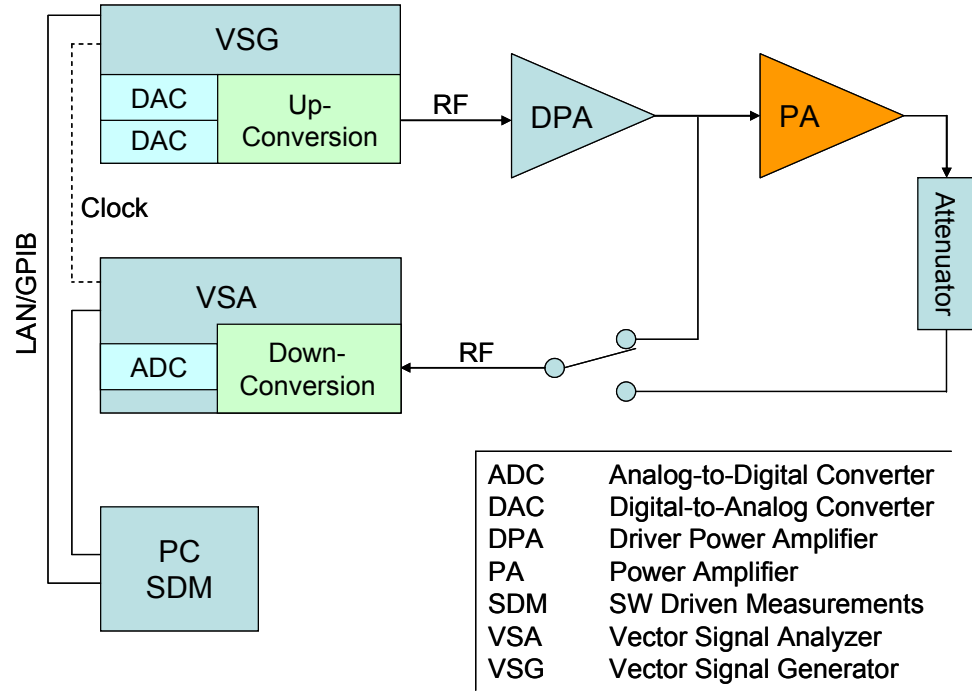
Fig. 5. The measurement system. The system is controlled by the PC where the SDM methods reside. Test signals are generated by the VSG and the input and output signals of the PA are captured by the VSA.

4.3 Software and Hardware Architecture

One important aspect of a measurement system such as the one in Fig. 5 is the software architecture used in the PC. It is most desirable that the instruments can be easily replaced depending on the hardware requirements for the application at hand, the availability of new instrumentation and so on. The idea is that the measurement functionality resides in the PC and that this measurement functionality is encapsulated in such a way that it is not dependent on the actual VSG or VSA that are present in the specific measurement set-up. This concept is also called SDM - software driven measurements. One attempt to design such a software architecture was proposed in [Paper L]. It is based on a layered architecture where the measurement functionality, or virtual instruments (VIs) (sometimes also called "synthetic instruments" (SIs)), resides in software components that communicates with the physical hardware through intermediary software layers.

A similar approach for the limited case of the LSNA that was introduced in Ch. 3 was taken in [36].

The current VI/SI trend goes toward a generic hardware/software platform as is further discussed in [37]. A typical example of a general VI/SI measurement system is shown in Fig. 6. It has been taken from [37] and is similar to the hardware architecture promoted by the Interchangeable VI foundation [38]. The concept is also further developed by measurement instrumentation vendors, e.g. [39].

The system is controlled by the PC and can generate a flexible number of RF output signals, a flexible number of analog baseband output signals and a flexible number of digital output signals. These are applied to the device under test (DUT) through a switch matrix. Similarly, on the receiver side the outputs of the DUT are sent to the appropriate receiver chain. Data handling and signal processing may be done using ASICs, FPGAs or DSPs. The SDM methods might reside in the PC or in the ASICs, FPGAs or DSPs. Despite the advanced hardware set-up of Fig. 6, the main part of the measurement is, again, the software, where the functionality resides as is described in [Paper L]. The hardware architecture is further discussed in [37].
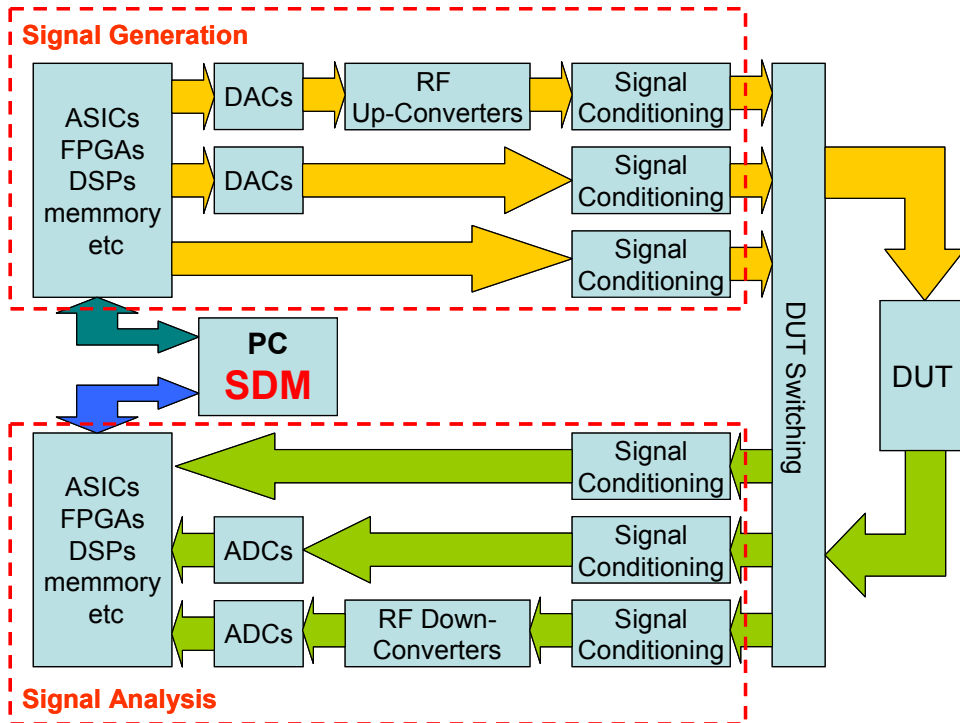
Fig. 6. A typical VI/SI measurement set-up [37]. The signal generation side can have any number of digital, analog and RF signal paths. Similarly the signal analysis side can receive any number of digital, analog and RF signals.

28

4.4 Experimental

With this kind of measurement system AM/AM and AM/PM plots, on sample basis, similar to what was shown in Fig. 1, Fig. 2 and Fig. 4 can be made. Such AM/AM and AM/PM plots are sometimes referred to as *dynamic* AM/AM and AM/PM [40] plots since they incorporate frequency dependence in the PA. The coordinates (x,y) in these plots are given by

$$\left(20 \log_{10} \left(|u(n)| \right), 20 \log_{10} \frac{|y'(n)|}{|u(n)|} \right)_{AM/AM} \tag{3}$$

$$\left(20 \log_{10} (|u(n)|), \angle u(n) - \angle y'(n) \right)_{AM/PM} \tag{4}$$

Such plots are shown in Fig. 7, AM/AM, and Fig. 8, AM/PM, for different average input power levels using a wideband (~4 MHz) modulated signal and a 40 W class-AB LDMOS PA. These plots have been taken from [Paper J].

In this specific measurement it is observed that for a low input power level (magenta) there is almost no spread in the AM/AM and AM/PM curves indicating negligible linear memory effects in the PA. As the power is increased, the spread does also increase, indicating a quite substantial amount of nonlinear memory effects. As the PA goes into compression (blue), the nonlinear memory effects in the peaks for AM/AM decreases, as can be expected. The PA cannot deliver more power, the history does no longer matter.

Fig. 7. Dynamic AM/AM plots for different input power levels.

Fig. 8. Dynamic AM/PM plots for different input power levels.

30

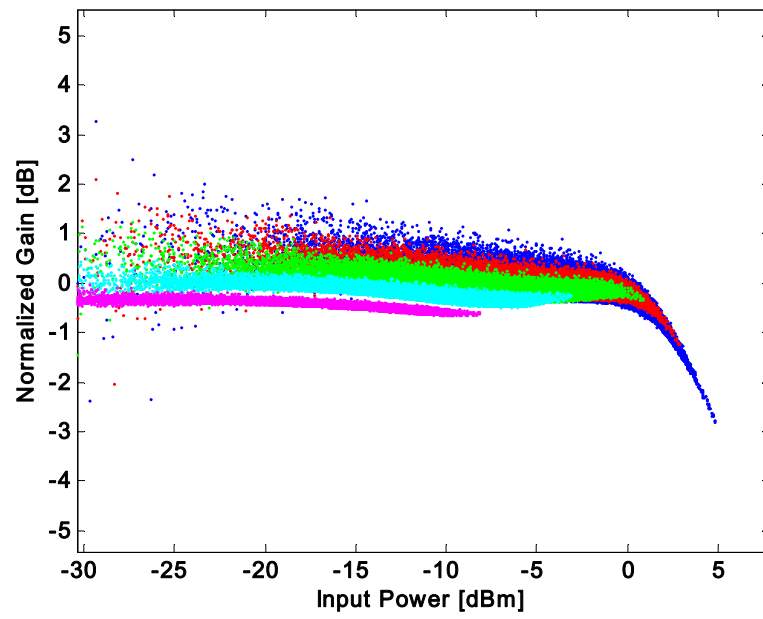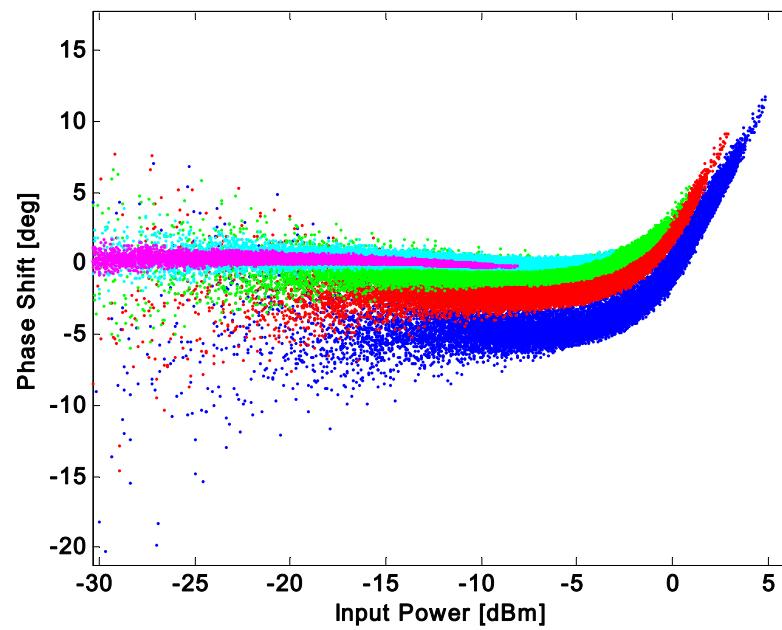# 5 Methods for Enhanced Measurement Performance

The main focus of this thesis has been to develop measurement methods and techniques in order to increase the raw performance of the hardware. Here we divide these techniques into three sub-groups depending on the performance parameter they are targeting, dynamic range, bandwidth or linear distortion. Techniques for extension of the dynamic range are treated in Ch. 5.1, techniques for bandwidth extension are treated in Ch. 5.2 and techniques to overcome the linear distortion are treated in Ch. 5.3.

Here it is chosen to describe a measurement system with an IQ-modulator based VSG and an intermediate frequency (IF) sampling based VSA. This choice is based on the discussion in [Paper G] and [32] and it gives a desirable trade-off between dynamic range and bandwidth. An overview of the main limitations and distortion mechanisms in the measurement set-up are given in Fig. 9, see [32] for a detailed discussion on the effects caused by these.

On the signal generation side there are numerous sources of distortion and limitations. There are a limited number of bits in the DACs, a limited clock frequency in DACs, an unequal gain between the I- and Q-paths in the VSG, a DC offset on the I- and/or Q-paths, nonlinear distortion in the I- and/or Q-paths, linear distortion in the I- and/or Q-paths, not a 90 degree phase shift between the I- and Q-paths, linear distortion when combining the I- and Q-paths, nonlinear distortion in VSG PA, nonlinear distortion in the DPA, numerous noise sources.

On the VSA side there is a limited sampling rate in the ADC, a limited number of bits in the ADC, linear distortion in the resolution bandwidth filter (RBW), noise.

Together the abovementioned factors settle the performance of the measurement system in terms of bandwidth, dynamic range and linear distortion.
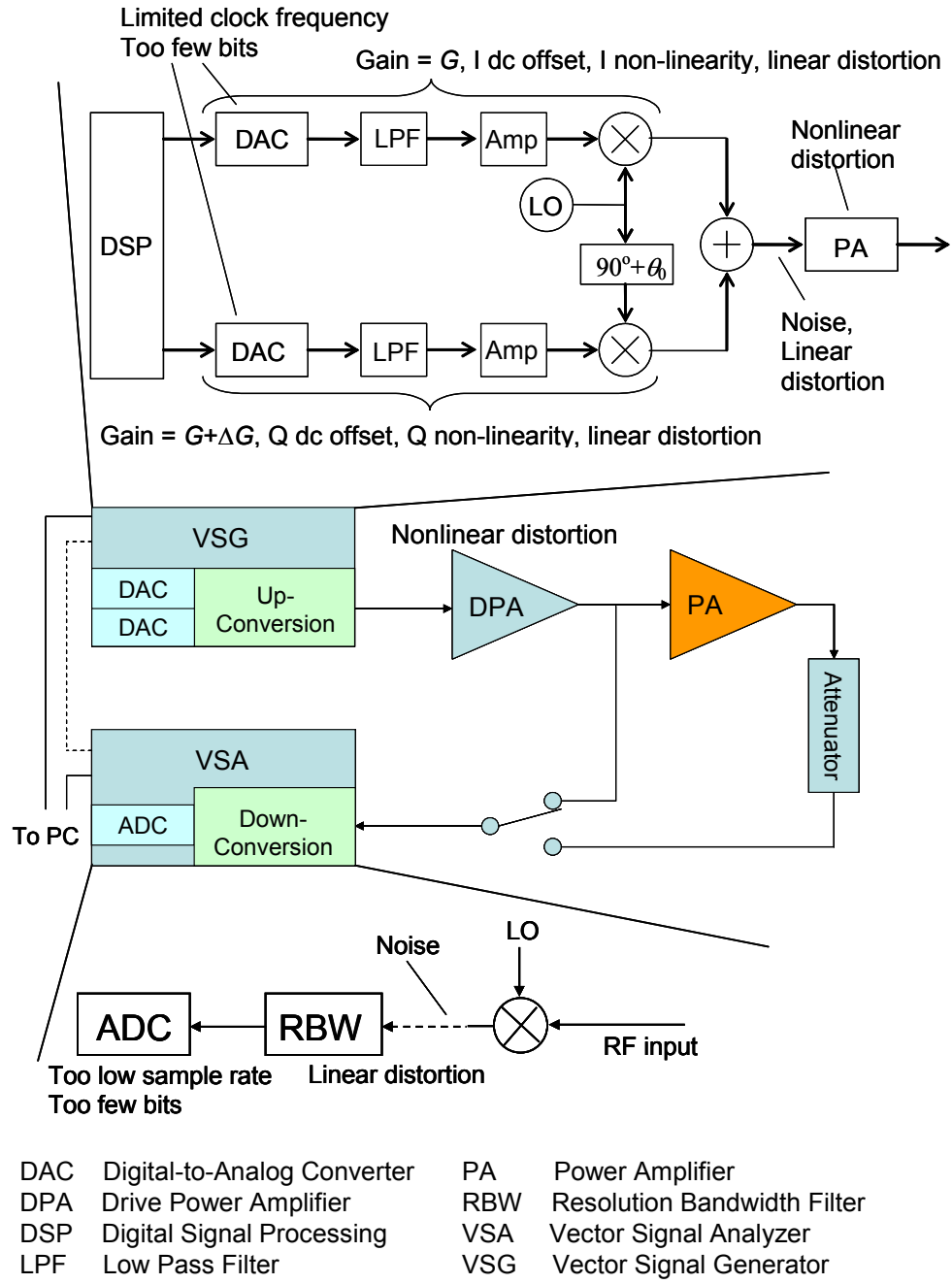
Fig. 9. Imperfections and distortion mechanisms in the measurement system. Both the VSG and the VSA contains numerous hardware limitations and distortions. The effects of these are studied in some detail in [32].

32

5.1 Extension of the Dynamic Range

The dynamic range of the measurement system is set by the noise and the nonlinear distortion. The highest dynamic range DR_{max} is obtained at the power level P_0 were they contribute equally, see Fig. 10. A measurement system of this kind is very weakly nonlinear and, thus, dominated by third order nonlinear effects. Hence, the distortion products can be expected to rise three dB as the power level is increased by one dB.

Three techniques have been used in this work in order to extend the dynamic range of the measurement system, *i*.) measurement of the input and output signals using the same receiver (VSA), *ii*.) coherent averaging of multiple measurements of the same signal and *iii*.) DPD of the DPA, see Fig. 9.

By measuring both the input and output signals of the PA, distortion products generated in the VSG will become a part of the input signal to which the output signal is compared. That is, the model identification will not be carried out using the intended ideal input signal, but with a signal that much more closely resembles the actual input signal to the PA, which is somewhat distorted. This essentially means that the distortion in the VSG will cancel between the measurements of the input and output signals and will not disturb the measurement.

Coherent averaging of multiple measurements of the same signal in order to decrease the noise is treated in [41] and [Paper E] and essentially means that the same test signal is measured several times, the measurements are then time-aligned and added together. This increases the effective dynamic range by $20\log_{10}(N)/3$ dB, where N is the number of measurements, as explained in [Paper E]. The averaging can only decrease the noise floor, the distortion will not be affected. If an even larger dynamic range is needed an RF bandpass filter can be placed directly after the VSG. An example of how the dynamic range can be extended through the use of coherent averaging and filtering was presented in [41] and an illustration of the typical performance improvement that can be expected from coherent averaging and filtering is shown in Fig. 11. The measurement is done with a ~4 MHz wide WCDMA like signal. The raw performance of the measurement system (No averaging) is shown in blue. With averaging in the VSA the effective dynamic range is increased with some 15 dB using 800 averages (Red). The dynamic range is now limited by the distortion in the VSG and cannot be further reduced using averaging. Instead a sharp ~4 MHz wide bandpass filter is used at the output of the VSG. The dynamic range is now further increased with some 10 dB to an excellent 90 dB in terms of ACLR as defined in [23] for WCDMA signals (Green).
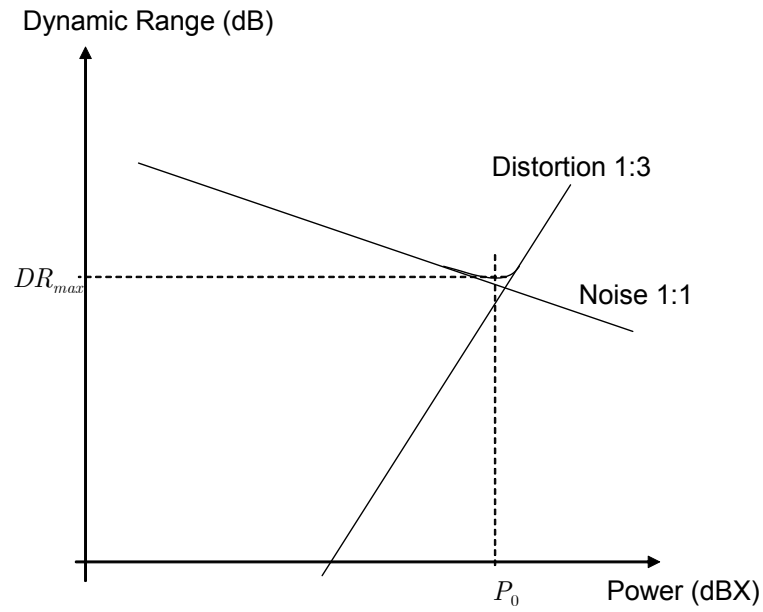
Fig. 10. Definition of maximum dynamic range in the measurement system.
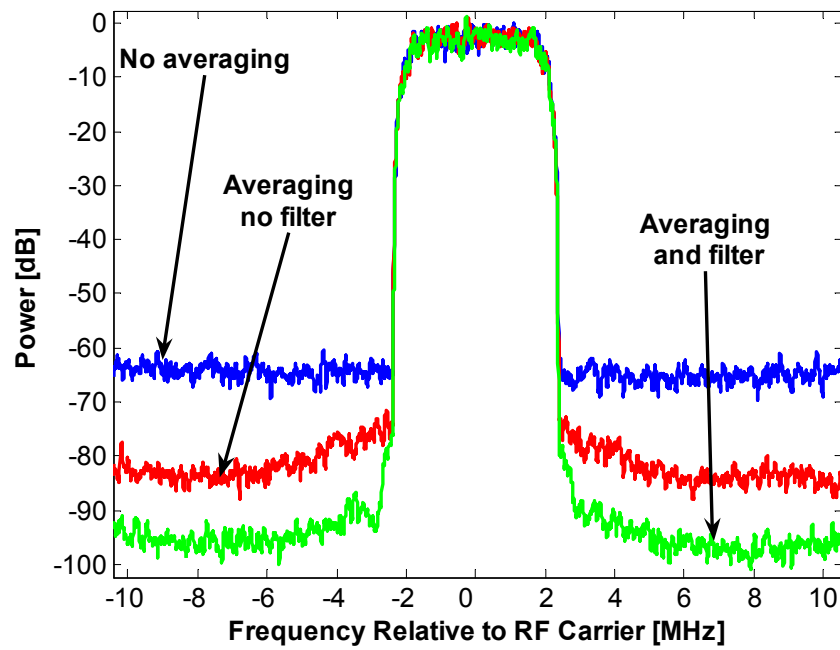
Fig. 11. The effects of filtering and averaging on a typical modulated signal.

34

When testing PAs that require a high input drive level, i.e. one-stage high power PAs, a DPA is needed as was shown in Fig. 5. In such cases the DPA may also contribute to the overall distortion. An alternative to put an RF filter after the DPA or to use an excessively large DPA is to apply DPD on the DPA in order to linearize it as was done in [Paper H]. An example of the performance that can be obtained is shown in Fig. 12 for an average output power level of approximately 33 dBm. This is enough for many basestation applications and could be further increased if needed.

If a highly distortion free input signal to the PA, or some other component, is desired the VSG may also need to be predistorted. Analysis and DPD and distortion phenomena in VSGs are somewhat treated in [32].
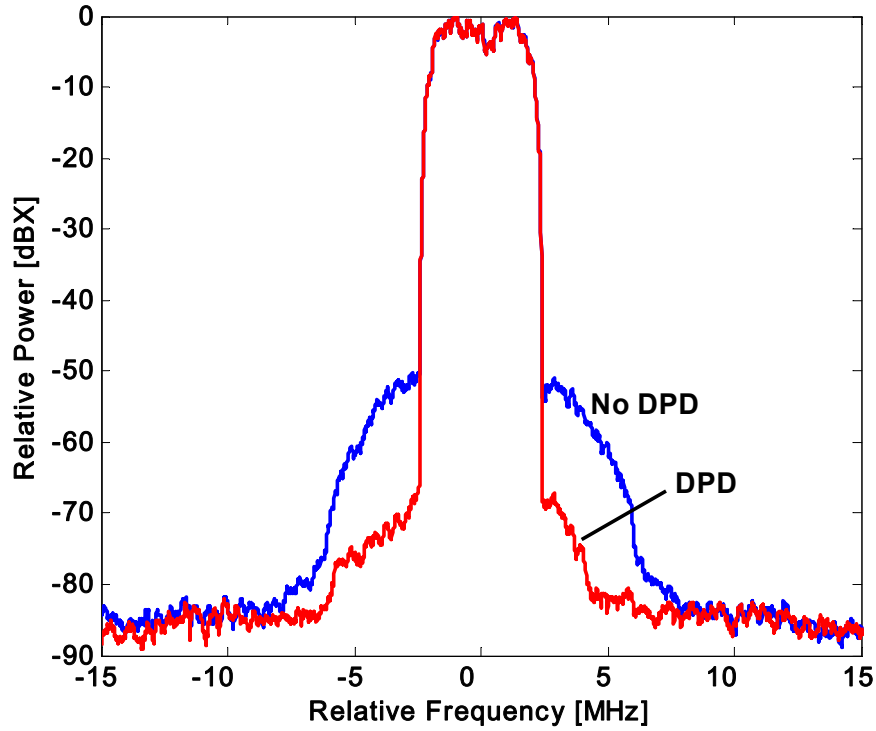
Fig. 12. The effect of DPD of the DPA.

5.2 Extension of the Measurement Bandwidth

The bandwidth of telecommunication systems have increased over the last ten, twenty years and may continue to do so [42], [43], [44], [45]. Further, it can be of interest to jointly amplify signals from different systems and bands in one PA. Thus, if efficiently and cheaply done, there is basically no limit to the bandwidth

requirements of the PA. In addition, and maybe more important from a short term measurement system view, the output signal of a nonlinear PA, due to the nonlinearities, has a considerably larger bandwidth than the input signal. A typical example could be that the input signal has a bandwidth of 20 MHz and while the bandwidth of the output signal might be more than 100 MHz. The bandwidth is here somewhat loosely defined but is essentially the frequency range for which the distortion raises above the noise floor. This is illustrated in Fig. 13.

This has consequences for the measurement system. While the bandwidth of the measurement system might be more than enough for measurement of the input signal, it can be completely insufficient for measurement of the output signal.

There is a trade-off between bandwidth and dynamic range, i.e. the number of bits in the ADC and the sampling frequency. They cannot both be maximized simultaneously.

Techniques to extend the available measurement bandwidth have been published. These techniques include interleaved ADCs first proposed in [46] and filter bank techniques described in e.g. [47].

The technique with interleaved ADCs is commonly used today in e.g. sampling oscilloscopes. The drawback with interleaved ADCs is that there is a timing mismatch between the different ADCs (two or more) which causes distortion. This distortion can however be compensated for, see e.g. [48].
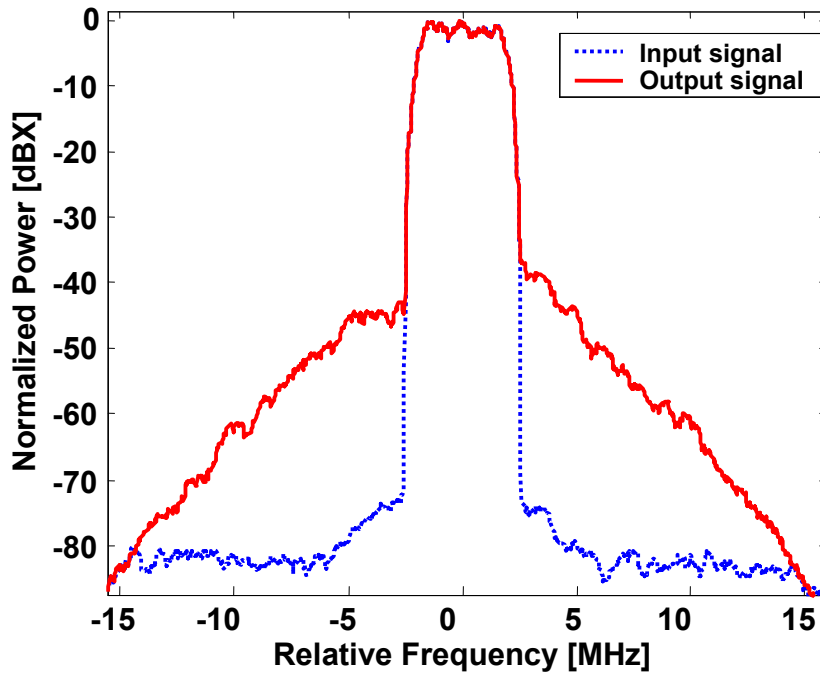
Fig. 13. Illustration of the bandwidth of typical input and output signals of the PA.

36

The filter bank technique uses a number of filters that filters out different parts, in frequency, of the signal. The output of each filter is then digitized. A sampled version of the signal is finally constructed in the digital domain.

In this work two other techniques are proposed for the application of PA characterization. These are the frequency stitching technique [Paper E] and the application of Zhu's generalized sampling theorem (ZGST), first proposed in [49], [Paper I] and [Paper K]. None of these are truly new, the frequency stitching technique is a tuning of the filter bank technique for the specific problem of PA characterization and ZGST is well known and have been discussed in conjunction with PAs for some time, see e.g. [50, 51], but seldom applied to real measurements.
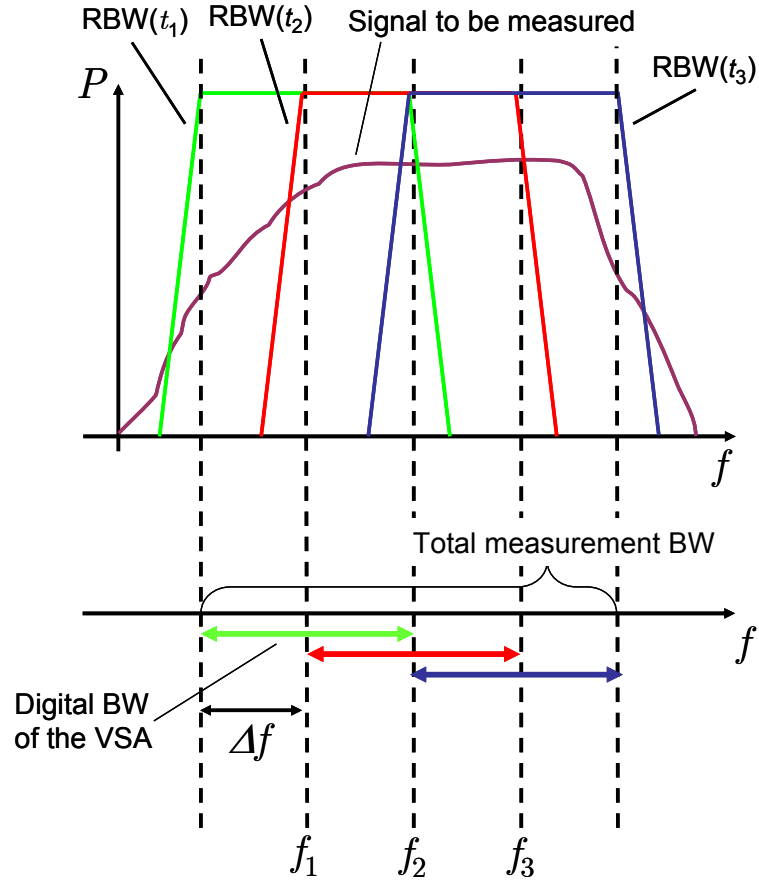
Fig. 14. The frequency "stitching" technique. Frequency "slices" of a wideband signal are measured at different time instances, t_1, t_2, ..., and centre frequencies f_1, f_2, ... The wideband signal is then reconstructed from these measurements.

As for the coherent averaging in Ch. 5.1, the frequency stitching technology is based on that a repetitive measurement signal is used. If the input signal to the PA is repetitive, the distorted output signal will also be repetitive. Since the signal is repetitive different parts of it, in the frequency domain, can be measured at different times using a narrowband receiver. The combined wideband signal can then be restored in the frequency domain. The frequency stitching technique is illustrated in Fig. 14.

ZGST essentially says that under some mild conditions the output signal of a nonlinear system can be reconstructed by sampling it at the Nyquist rate of the input signal rather than the Nyquist rate of the output signal. The required conditions are essentially that the input and output signals are band-limited and that the nonlinear system performs a one-to-one mapping of the input signal to the output signal. These conditions are normally met in practice for PAs. Somewhat more detailed discussions on the conditions and their fulfillment for PAs have appeared in [52] and [53].

Here we note the potential of the ZGST while some measurement results are presented in [Paper I] and [Paper K]. The ZGST is also somewhat discussed in Ch. 6 in conjunction with PA modeling. The results are essentially that the ZGST can be used without loss of performance.

5.3 Correction of Linear Distortion

Most authors tend to neglect the influence of the linear distortion in the measurement set-up, probably partly because, to the author's knowledge, no simple calibration technique has been proposed until recently. Especially the phase calibration pose a problem.

Measurement systems of the kind shown in Fig. 5 suffer from linear distortion both in the VSG and the VSA as was described above, see again Fig. 9. Especially the linear distortion in the VSA can cause problems. The linear distortion in the VSG will cancel similarly to the nonlinear distortion from the VSG, as was described in Ch. 5.1, provided that both the input and output signals of the PA are measured. The linear distortion in the VSA, mostly caused by the RBW, on the other hand, will only cancel between the two measurements to some degree. Especially the out-of-band distortion in the output signal will to some extent be filtered, see Fig. 15.

In addition to what is said above the linear distortion in the VSA will be the dominant error contributor when the frequency stitching method in Ch. 5.2 is used, as was described in [Paper E].

38
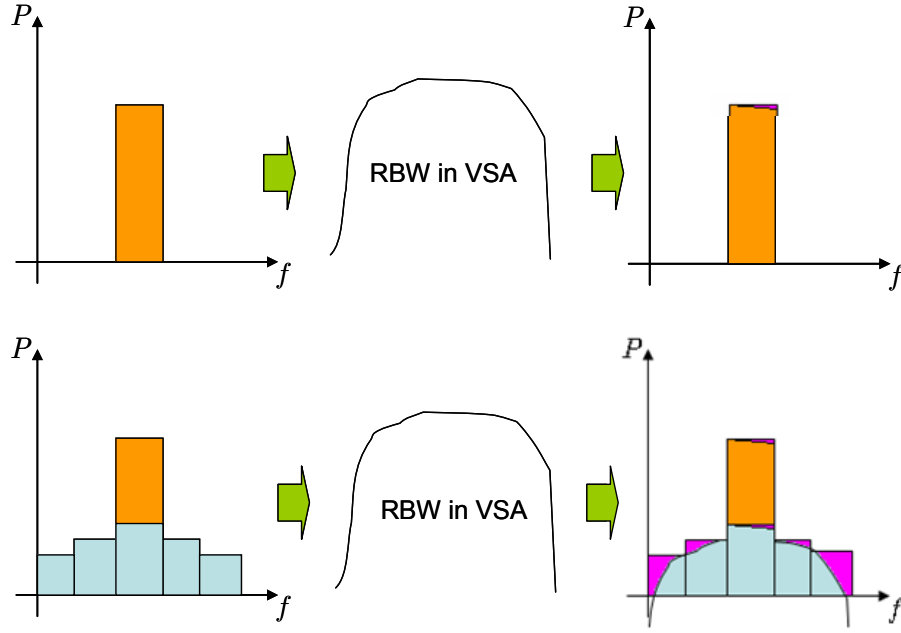
Fig. 15. The effects of linear distortion in the VSA on the input and output signals of the PA. While the input signal and the in-band distortion are only marginally affected the out-of-band distortion is often significantly distorted by the RBW.

A technique to calibrate both the amplitude and the phase of both the VSA and the VSG without using extra instrumentation, which also works together with the frequency stitching technique that was described in [Paper E], is proposed in [Paper F]. The basic principle for the technique proposed in [Paper F] is that the VSG is first connected directly to the VSA. Then multiple measurements are taken while changing the center frequency of either the VSG or VSA slightly. This will generate the necessary calibration information.

Another technique to calibrate the linear distortion would be to first calibrate the VSG for amplitude and phase using a DSO which has negligible distortion over the bandwidth of a typical VSG. Then, using the calibrated VSG, the VSA can be calibrated.

Yet another method was proposed in [54] in which the phase response of a DSO is found from the amplitude response using the Hilbert transform. A direct approach of such a method gives large errors [32]. In [54] these errors are approximated using a small number of basis functions in order to obtain a more accurate result. A similar approach could most likely be taken also for the case of VSG/VSA calibration.

Similar calibration problems are also encountered in the calibration of LSNAs, see Ch. 3 [55].

6 Complex Envelope Behavioral PA Modeling

6.1 Introduction

With complex envelope behavioral PA modeling is here meant a model that models the PAs influence on the complex envelope of the signal as it passes through the PA. It is a black box model in the sense that it has no explicit connection to any physical quantity and it is not known what happens inside the PA. The interest here is simply to construct an input – output mapping for the complex envelope of the signal in the first spectral zone as it is passed through the PA.

This is in contrast to other kinds of behavioral PA models that try to model the entire behavior of the PA, not only the behavior in the first spectral zone.

Complex envelope models are even further different from physical models where the focus is on the physical parameters, e.g. currents, impedances, etc.

If (2) is input to the amplifier, the output in the first spectral zone, after sampling, is given by

$$y(n) = K(u(n)), \qquad (5)$$

where $K(\cdot)$ is the complex envelope response of the PA in the first spectral zone that are to be modeled. Some such models are studied in Ch. 6.

An important property of a modulated signal that is to be used for characterization of PAs is its PAPR. The PAPR is the maximum of the instantaneous power envelope defined by $p(n) = |y(n)|^2$, divided by the average power. It is most often expressed in dB. It essentially sets the amplitude range of the characterization. Typically PAPR values of 6-9 dB are encountered in many communication systems. Numerous techniques exist to decrease the PAPR for different kind of signals. This is of interest since a low PAPR enables higher efficiency in the PA. Two kinds of signals that are of particular interest is multiple tone signals, as they are often used for PA characterization, see e.g. [56] and [57], and orthogonal frequency division multiplexing (OFDM) signals as they are used in modern communication systems. See e.g. [58], [59], [60] and [61] for techniques of PAPR reduction for multiple tone signals and [62] and [63] for some PAPR techniques for OFDM signals.

In Ch. 6.2 goodness criteria for evaluation of behavioral complex-envelope PA models are discussed and in Ch. 6.3 some such models are treated.

6.2 Goodness Criteria for Evaluation of PA Models

The main goodness criteria used in this work are the normalized mean-square error (NMSE) and adjacent channel error power ratio (ACEPR). The exact definitions of these have varied somewhat between different papers and do also differ between different authors. Here the following definitions are used:

$$\text{NMSE} = 10 \log_{10} \left(\frac{\varepsilon}{\sum_n |y_{meas}(n)|^2} \right), \qquad (6)$$

$$\text{ACEPR} = \max_{i=1,2} \left\{ \frac{\int_{(adj)_i} |E(f)|^2 \, df}{\int_{ch} |Y(f)|^2 \, df} \right\}, \qquad (7)$$

where ε is defined as

$$\varepsilon = \sum_n |y_{meas}(n) - y'_{sim}(n)|^2 \quad , \qquad (8)$$

where $y'_{sim}(n)$ is an amplitude and time adjusted version of the original output signal of the model $y_{sim}(n)$, such as ε is minimized. This is in agreement with the error calculation procedures in the ETSI standard [23]. Further, $y_{meas}(n)$ is the measured output signal, $Y_{meas}(f)$ and $Y_{sim}(f)$ are the time-discrete Fourier transforms (TDFTs) of $y_{meas}(n)$ and $y_{sim}(n)$, respectively, and $E(f)$ is the TDFT of $e(n) = y_{meas}(n) - y'_{sim}(n)$. The integrals in (7) are taken over the 3.84 MHz wide channel ch and the two adjacent channels adj, centered 5 MHz above and below the channel, respectively, as defined in the ETSI standard [23] for the 3G system WCDMA. In principle, similar criteria for out-of-band emissions can be defined in the frequency domain for other standards as well. The ACEPR is illustrated in Fig. 16, where the TDFT of $u(n)$, $U(f)$, is also shown.

The NMSE is a measure of the total model error, which is of obvious interest when designing a model. A problem with the NMSE, however, is that it is in most cases completely dominated by the error inside the channel, see again Fig. 16. The ACEPR, by definition, is a measure of the out-of-band error, which in many cases, is of higher interest than the in-band error as given by the NMSE. It is the out-of-band distortion that is generated in the adjacent channels that disrupts communications in other channels while the communication inside the channel will be at most marginally affected by the nonlinear distortion in the PA.

Thus, the combination of NMSE and ACEPR is believed to be a reasonable

42

goodness criterion on which different behavioral PA models, but also other kinds of PA models can be judged.

Some other criteria have been proposed in the literature, see e.g. [64] in which the memory effect ratio (MER) was proposed. The MER is essentially defined as the ratio of rms error that cannot be modeled with a memoryless model to the rms value of the output signal.

There is an ongoing discussion on evaluation criteria for behavioral PA models of the kind discussed here. An attempt to contribute to that discussion was presented in [65].
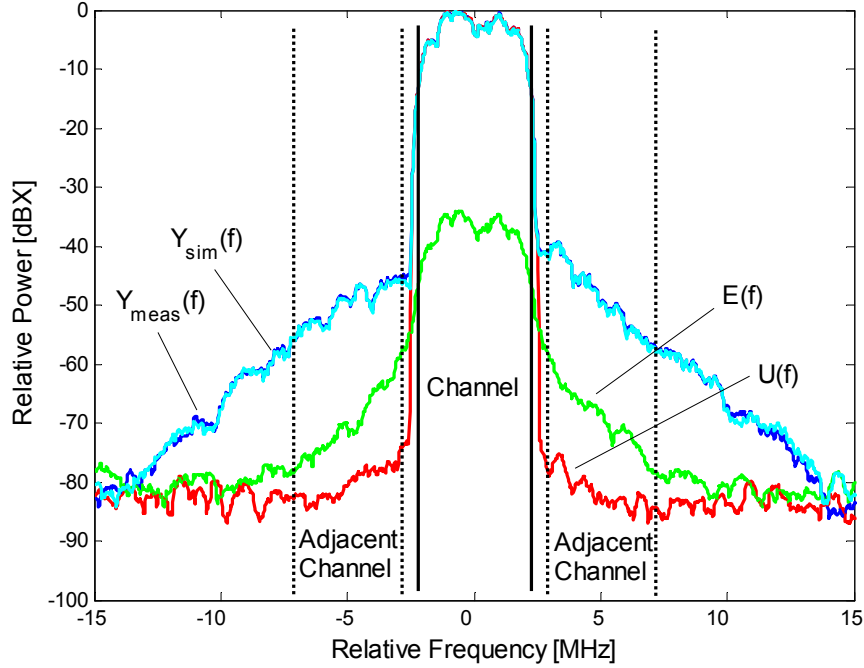
Fig. 16. Definition of the channel and the adjacent channel for WCDMA signals according to [23].

6.3 Some Complex Envelope Behavioral PA Models

Numerous complex envelope behavioral PA models have been proposed and it is certainly beyond the scope of this work to cover them all. A comprehensive overview of some of the most important can be found in [66].

One of the simplest models of this kind is the complex polynomial model given by

$$y(n) = K(u(n)) = \sum_{p=1}^{P} a_{2p-1} |u(n)|^{2(p-1)} u(n) \qquad (9)$$

where the a_i:s, $i = 1, 3, ..., 2P$-1, are the complex-valued parameters that are to be determined.

This model does however not take any frequency dependence, or "memory effects" in the PA into account and, thus, share most of the shortcomings of the more traditional techniques in Ch. 2.

Severely more complicated models have been proposed. Many of them do also posses general approximation capabilities. That is, they can essentially approximate any continues function, thus, they can also approximate the response of a nonlinear PA, at least in theory. Among these models are neural network models, see e.g. [67], [Paper A], Volterra series [68] with variants, e.g. the Kautz-Volterra model [69] and block oriented models such as the parallel Wiener model [15].

A problem for the Volterra and neural network models is that they suffer from slow convergence due to the many parameters that have to be determined. The Kautz-Volterra and the parallel Wiener models, on the other hand, suffer from complicated system identification procedures. In practice considerable simpler models have been shown to have equal or better performance with regard to NMSE, and especially ACEPR, in many, not to say most, practical cases. One such model, with particularly good performance with regard to ACEPR, is the parallel Hammerstein (PH) or tapped delay line model. The PH model was first proposed for amplifier modeling in [70], and is now widely used both for modeling and DPD of PAs, see e.g. [64], [71], [72]. The structure of the PH models is shown in Fig. 17. Mathematically the PH model is given by

$$
\begin{aligned}
y(n) &= \sum_{p=1}^{P} H_{2p-1}(q^{-1}) |u(n)|^{2(p-1)} u(n) = \\
&\quad \sum_{p=1}^{P} \sum_{m=0}^{M} b_{m,2p-1} |u(n-m)|^{2(p-1)} u(n-m) \,,
\end{aligned}
\qquad (10)
$$

where the contributions of different nonlinear orders, e.g. three, five etc, are filtered by different filters $H_i(q^{-1})$ having the complex-valued coefficients $b_{j,i}$, $i = 1, 3, ..., 2P$-1, $j = 0, 1, 2, ..., M$ and q^{-1} is the delay operator.

Despite some shortcomings such as a somewhat higher NMSE than some other models, e.g. the neural network and Kautz-Volterra models, the PH model must currently, due to its simplicity and generally good performance in many practical situations, be considered as the baseline to which other proposed complex envelope behavioral PA models should be compared.
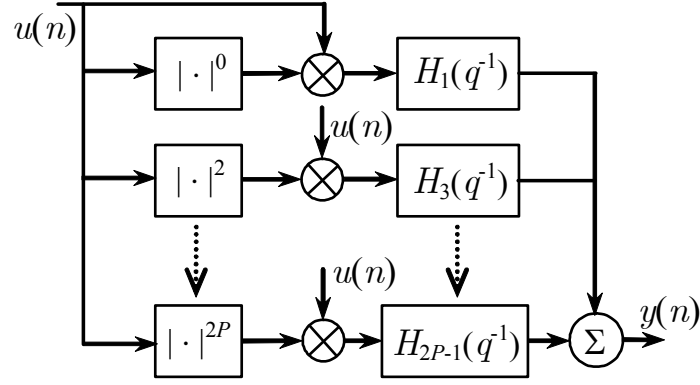
44

Fig. 17. The PH model. Each nonlinear order is filtered through a linear filter.

In this work some model development has also been done.

In [73] a neural network model was proposed and subsequently extended with regard to bandwidth in [Paper A] using the frequency stitching technique that was described in Ch. 5.2. The primary advantage of the proposed neural network model over the PH model is its lower NMSE. Its drawback is its higher ACEPR.

In [Paper B] different models, including the proposed neural network model and the PH model were compared. This paper is maybe the only published attempt to experimentally compare an array of different PA models for several different input signals, different PAs, different bandwidths and different power levels. All in all the paper is based on ~7000 PA model identification and validations based on measured data. The results basically confirmed the usefulness of the PH model. A second result was the weak generalization capabilities of the PH (and other) models with respect to power level and bandwidth. As a result, it was proposed in [Paper J] to include the average power level in the PH model in order to increase its generalization properties. An alternative would be to incorporate the very long term, i.e. thermal, memory effects [24], [74] into the model using techniques similar to the one presented in [75].

As already discussed in Ch. 5.2, it was proposed in [Paper I] and [Paper L] to apply ZGST to PA modeling as an alternative technique to extend the measurement bandwidth. ZGST was used in conjunction with the PH model and it was found that the ZGST is indeed very useful since the sampling rate can essentially be lowered from the Nyquist rate of the output signal to the Nyquist rate of the input signal with negligible loss in modeling performance.

7 Summary of Appended Papers

The author has contributed in all parts of all the listed papers except Paper C, where the contribution is limited to the experimental part and some discussions and manuscript proofreading. The papers [Paper A] and [Paper B] are joint works where the first author has contributed most but this author has taken part in all aspects of the work and been responsible for some, e.g. experimental.

7.1 Paper A

M. Isaksson, D. Wisell, and D. Rönnow, "Wideband Dynamic Modeling of Power Amplifiers Using Radial-Basis Function Neural Networks," *IEEE Trans. Microwave Theory and Tech.*, vol. 53, pp. 3422-28, 2005.

A radial-basis function neural network (RBFNN) has been used for modeling the dynamic nonlinear behavior of an RF power amplifier for 3G. In the model the signal's envelope is used. The model requires less training than a model using IQ-data. Sampled input and output signals were used for identification and validation. Noise-like signals with bandwidths of 4 MHz and 20 MHZ were used. The RBFNN is compared to a parallel Hammerstein (PH) model. The two model types have similar performance when no memory is used. For the 4 MHz signal the RBFNN has better in-band performance, whereas the PH is better out-of-band, when memory is used. For the 20 MHz signal the models have similar performance in- and out-of-band. Used a as a digital predistortion algorithm the best RBFNN with memory suppressed the lower (upper) adjacent channel power 7 dB (4 dB) compared to a memoryless nonlinear predistorter and 11 dB (13 dB) compared to the case of no predistortion, for the same output power for a 4 MHz wide signal.

7.2 Paper B

M. Isaksson, D. Wisell, and D. Rönnow, "A Comparative Analysis of Behavioral Models for RF Power Amplifiers," *IEEE Trans. Microwave Theory Tech.*, vol. 54, pp. 348-359, 2006.

A comparative study of nonlinear behavioral models with memory of radio frequency power amplifier (PAs) is presented. The models are static polynomial, parallel Hammerstein (PH), Volterra, and radial basis-function neural network (RBFNN). Two PAs were investigated, one designed for the 3G mobile telecommunication systems and one for 2G. The 2G PA was found to have

larger memory effects than the 3G PA. A Volterra model was better than a PH for the same nonlinear order and memory depth. The best PH was better than the best Volterra model, since the former can be identified with higher nonlinear order and memory depth. The RBFNN reduced the total model error slightly more than the PH, but the error out-of-band was significantly lower for the PH. The qualitative conclusions are the same for the 2G and 3G PAs, but the model errors are smaller for the latter. For the 3G PA, a static polynomial was as good as the best PH and better than the RBFNN for the hardest cross-validation (identification with a noise signal, validation with an eight tone signal). The models with memory, PH and RBFNN, showed better cross-validation performance than a static polynomial for the hardest cross-validation for the 2G PA.

7.3 Paper C

D. Rönnow, D. Wisell, and M. Isaksson, "Three-Tone Characterization of Nonlinear Memory Effects in Radio Frequency Power Amplifier." *To appear, IEEE Trans. Instrum. Meas.*

A stepped three-tone measurement technique based on digitally modulated baseband signals, is used for characterizing radio frequency power amplifiers. The bandwidth of the stepped measurement was 8.8 MHz for the input and 26.4 MHz for the output signal. A power amplifier designed for third-generation mobile telecommunication system was analyzed. The amplitude and phase of the third-order Volterra kernel were determined from identified intermodulation products. The properties of the Volterra kernel along certain paths in the three-dimensional frequency space were analyzed and compared to some box-models for nonlinear systems. The main symmetry of the third-order Volterra kernel of this power amplifier was found to be of the type given by cascaded quadratic nonlinearities with a linear filter between (a Hammerstein-Wiener system) and the frequency dependence, i.e. memory effects, was found to be due to effects at baseband.

7.4 Paper D

D. Wisell, B. Rudlund, and D. Rönnow, "Characterization of Memory Effects in RF Power Amplifiers Using Digital Two-Tone Measurements," *To appear, IEEE Trans. Instrum. Meas*.

In this paper a novel method to measure the amplitude and phase of two-tone third order intermodulation products generated in a high-power amplifier is presented. The method is based on the sampled input and output signals of the amplifier. The presented measurement set-up and the associated algorithms for calculation of the amplitudes and phases are considerably faster and simpler than

current methods. By making use of the sampled input and output signals of the amplifier and signal processing techniques, the need for a non-linear reference, a tunable attenuator and a phase shifter, reported in existing measurement set-ups are eliminated, making it simple and easy to use. Hence, this is a substantial simplification of the measurement set-up compared to what have been reported earlier. The proposed measurement set-up is also suitable for fast, automated measurements, which is of interest for many applications, both lab and production oriented. In addition, a method to increase the bandwidth of the measured signal is used to overcome the bandwidth limitation set by the Nyquist criteria for sampled systems. Measurements are done on two base station high-power amplifiers and are found to be in agreement with theory and reference measurements.

7.5 Paper E

D. Wisell, D. Rönnow, and P. Händel, "A Technique to Extend the Bandwidth of a Power Amplifier Test-bed," *IEEE Trans. Instrum. Meas.*, vol. 56, pp. 1488-1494, 2007.

In this paper a method for increasing the bandwidth of a test-bed for dynamic characterization of power amplifiers is described. The technique is readily implemented using commercially available instruments which makes it suitable for e.g. production testing. The bandwidth extension technique is combined with coherent averaging of the measurements in order to simultaneously increase the bandwidth and dynamic range of the test-bed. The errors in the obtained wideband signal are also estimated. The method is evaluated experimentally on a basestation power amplifier for the 3G WCDMA system and on a Doherty amplifier. A tenfold increase in bandwidth to a total of 144 MHz and a more than 10 dB increase in dynamic range to 78 dB were obtained in practice. In addition the obtained wideband signal is used for behavioral amplifier modeling.

7.6 Paper F

D. Wisell and P. Händel, "Simultaneous Measurement of Transmitter and Receiver Magnitude and Phase Ripple," *Submitted, Measurement, Jan 2007*.

This paper describes a method to simultaneously measure the magnitude and phase ripple of two band pass linear systems in cascade by changing the center frequency for one of the systems. Extensive measurements are presented to support the theory. The method has a wide applicability for measurements on RF power amplifiers, transmitters, receivers, etc. The accuracy of the method is in the order of a few hundredths of a dB and one degree for most realistic measurement set-ups.

7.7 Paper G

D. Wisell, "A Baseband Time Domain Measurement System for Dynamic Characterisation of Power Amplifiers with High Dynamic Range over Large Bandwidths," presented at IEEE Instrum. Meas. Tech. Conf., Vail, Colorado, 2003, pp. 1177-80.

This paper describes, and discusses in some detail, a measurement system for dynamic characterisation of power amplifiers. The system uses data that are generated and collected at baseband to accurately calculate AM/AM and AM/PM distortion as well as memory effects in the amplifiers. The limitations of the system in terms of dynamic range and bandwidth are discussed as well as techniques to overcome them. The system may serve as a tool both for designers of power amplifiers as well as for development of amplifier models and systems for pre-distortion.

7.8 Paper H

D. Wisell, M. Isaksson, N. Keskitalo, and D. Rönnow, "Wideband Characterization of a Doherty Amplifier Using Behavioral Modeling," presented at ARFTG 67, San Fransisco, 2006, pp. 190-99.

A Doherty amplifier was investigated using behavioral amplifier modeling techniques. A measurement system for simultaneous wide bandwidth (>100 MHz) and large dynamic range (~70 dBc ACLR) sampled measurements that are needed for the behavioral modeling is presented. Both the measurement system and the performance of the Doherty amplifier are described. The findings are that the well known and widely used parallel Hammerstein model, also denoted the memory polynomial model, is well suitable also for modeling and predistortion of Doherty amplifiers, and that a Doherty amplifier can be designed with only minor memory effects. This is seen in the modeling error, which is reduced by 13 dB, compared with a constant gain, using a memoryless polynomial model and only 6 dB further by adding memory to the model.

7.9 Paper I

D. Wisell, "Exploring the Sample Rate Limitation for Modeling of Power Amplifiers," presented at IMEKO 2006, Rio de Janeiro, 2006.

In this paper it is shown that for the purpose of nonlinear power amplifier behavioral modeling, the sampling rate can be set to the Nyquist rate of the input

50

signal, rather than to the Nyquist rate of the output signal by making use of Zhu's generalized sampling theorem. This claim is supported by measurements on a basestation power amplifier. The findings are that the model error obtained when the output signal is sampled at the Nyquist rate of the input signal is approximately 1.5 dB higher than when the sampling rate is set to the Nyquist rate of the output signal. However, if a sampling rate of twice the Nyquist rate of the input signal is used, which is still typically, much lower than the Nyquist rate of the output signal, the degradation is only 0.2 dB. These are important findings that will substantially ease the requirements on ADCs used in measurement set-ups used for amplifier modeling.

7.10 Paper J

D. Wisell and N. Keskitalo, "A Behavioral Power Amplifier Model that Includes the Average Power Level," presented at ARFTG 68, Boulder, CO, 2006.

In this paper a behavioral power amplifier model that incorporates the average input power level is proposed. The result is a model that can accurately predict the output signal of the amplifier for all input power levels. The model is validated using measurements on a radio base station power amplifier and it is found that it does indeed has improved generalization capabilities with regard to input power level compared to previous models.

7.11 Paper K

D. Wisell, P. Stenvard, A. Hansebacke and N. Keskitalo, "Considerations when Designing and Using Virtual Instruments as Building Blocks in Flexible Measurement System Solutions," presented at IEEE Instrum. Meas. Tech. Conf., 2007.

In this paper the software and hardware structure of a virtual instrument measurement system is discussed. The focus is on flexibility, modularity, generality and hardware independence. A software architecture that meets these requirements is proposed and discussed in some detail. The proposed software architecture has a layered structure that makes it suitable for implementation of versatile measurement systems. The measurement functionality is encapsulated in its own, hardware independent layer and communicates with its environment, e.g. physical hardware, through intermediary software components. Finally a measurement system for characterization of power amplifiers that is designed following the proposed software architecture, with software driven measurements, is implemented.

7.12 Paper L

D. Wisell and P. Händel, "Implementation Considerations on the Use of Zhu's General Sampling Theorem for Characterization of Power Amplifiers," presented at IEEE Instrum. Meas. Tech. Conf., 2007.

In this paper Zhu's generalized sampling theorem for sampling of the output signal of a nonlinear system is applied to the case of radio frequency power amplifier modeling. The paper deals in some detail with hardware implementational issues in order to optimize the hardware design in order to make full use of the benefits given by Zhu's generalized sampling theorem. It is shown that some design changes have to be done compared to more traditional receiver designs, such as removing the anti-aliasing filters. It is also shown that the behavioral amplifier models that are extracted using data taken using Zhu's generalized sampling theorem have equal or better performance with regard to out-of-band spectral emissions than when the models are extracted using data taken using Nyquist sampling of the output signal of the amplifier.

References

[1]   B. Berglund, M. Englund, and J. Lundstedt, "Third design release of Ericsson's WCDMA macro radio base stations," *Ericsson Review*, pp. 70-81, 2005.

[2]   F. Raab et. al., "Power Amplifiers and Transmitters for RF and Microwave," *IEEE Trans. Microwave Theory Tech.*, vol. 50, pp. 814-826, 2002.

[3]   S. C. Cripps, *Advanced Techniques in RF Power Amplifier Design*. Boston: Artech House, 2002.

[4]   S. Boumaiza and F. M. Ghannouchi, "Realistic Power-Amplifier Characterization With Application to Baseband Digital Predistortion for 3G Base Stations," *IEEE Trans. Microwave Theory Tech.*, vol. 50, pp. 3016-3021, 2002.

[5]   A. Moulthrop, M. Muha, C. Clark, and C. Silva, "Baseband Time-Domain Waveform Measurement Method," US Patent 6,211,663, 2001.

[6]   O. Andersen, P. Malmlöf, and D. Wisell, "Nonlinear Characterization of Multiple Carrier Power Amplifiers," presented at ARFTG 56 2000, Boulder, CO, USA, 2000, pp. 151-58.

[7]   W. Bösch and G. Gatti, "Measurement and Simulation of Memory Effects in Predistortion Linearizers," *IEEE Trans. Microwave Theory Tech.*, vol. 37, pp. 1885-1890, 1989.

[8]   M. S. Heutmaker, J. R. Welch, and E. Wu, "Using Digital Modulation to Measure and Model RF Amplifier Distortion," *Applied Microwave & Wireless*, vol. 9, pp. 34 - 39, 1997.

[9]   Y. Yang, J. Yioongjin, N. B. Kim, and M. Park, "Measurement of Two-Tone Transfer Characteristics of High-Power Amplifiers," *IEEE Trans. Microwave Theory Tech.*, vol. 49, pp. 568-571, 2001.

[10]   N. Suematsu, Y. Iyama, and O. Ishida, "Transfer Characteristics of IM3 Relative Phase for a GaAs FET Amplifier," *IEEE Trans. Microwave Theory Tech.*, vol. 45, pp. 2509-2514, 1997.

[11]   U. Lott, "Measurement of Magnitude and Phase of Harmonics Generated

in Nonlinear Microwave Two-Ports," *IEEE Trans. Microwave Theory Tech.*, vol. 37, pp. 1506-1511, 1989.

[12]	A. Walker, M. Steer, and K. G. Gard, "A Vector Intermodulation Analyzer Applied to Behavioral Modeling of Nonlinear Amplifiers With Memory," *IEEE Trans. Microwave Theory Tech.*, vol. 54, pp. 1991-1999, 2006.

[13]	J. Vuolevi, T. Rahkonen, and J. Manninen, "Measurement Technique for Characterizing Memory Effects in RF Power Amplifiers," *IEEE Trans. Microwave Theory Tech.*, vol. 49, pp. 1383-1389, 2001.

[14]	K. Remley, D. Williams, D. Schreurs, G. Loglio, and A. Cidronali, "Phase Detrending for Measured Multisine Signals," presented at ARFTG 61, 2003, pp. 73-83.

[15]	H. Ku, M. D. McKinley, and J. S. Kenney, "Quantifying Memory Effects in RF Power Amplifiers," *IEEE Trans. Microwave Theory Tech.*, vol. 50, pp. 2843-2849, 2002.

[16]	K. Remley, D. Williams, D. Schreurs, and J. Wood, "Simplifying and Interpreting Two-Tone Measurements," *IEEE Trans. Microwave Theory Tech.*, vol. 52, pp. 2576-2584, 2004.

[17]	M. Schetzen, *The Volterra & Wiener Theories of Nonlinear Systems*. New York: Wiley, 1989.

[18]	S. Boyd, Y. Tang, and L. Chua, "Measuring Volterra Kernels," *IEEE Trans. Circuits Syst.*, vol. 30, pp. 571-577, 1983.

[19]	H.-C. Chang, S.-W. Chen, D. Moe, and S. Hackman, "CDMA ACPR Prediction Using Two-Tone Intermodulation Spectrum by Modeling Device Non-linearity with Tchebyshev Polynomials," presented at Wireless 1997, 1997, pp. 117-120.

[20]	W. Chen, J. Tsai, S. Chen, and T. Huang, "ACPR and IM3R Correlation of Broadband Signals in Microwave and Millimeter Wave Frequencies," presented at IEEE International Workshop on Radio-Frequency Integration Technology, Singapore, 2005, pp. 150-52.

[21]	H. Ku, M. D. Mckinley, and J. S. Kenney, "Extraction of Accurate Behavioral Models for Power Amplifiers with Memory Effects using Two-tone Measurements," presented at MTT-S, Seattle, 2002, pp. 139-142.

[22]	T. Goh, R. Pollard, and S. Boussakta, "ACPR Prediction of Multi-Carrier

Through Behavioural Modelling of Power Amplifiers Using Measured Two-Tone Transfer Characteristics and Statistical Techniques," presented at High Frequency Postgraduate Student Colloquium, 2002.

[23]   ETSI, "3GPP TS 25.141 latest rev."

[24]   J. H. K. Vuolevi and T. Rahkonen, *Distortion in RF Power Amplifiers*. Boston: Artech House, 2003.

[25]   N. Pothecary, *Feedforward Linear Power Amplifiers*. London: Artech House, 1999.

[26]   R. Davis and R. Boyd, "Adaptive Predistortion Technique for Linearizing a Power Amplifier for Digital Data Systems ", US Patent 4,291,277, 1981.

[27]   Agilent, "89604A Distortion Test Suite,", http://cp.literature.agilent.com/litweb/pdf/5988-7812EN.pdf, 2002.

[28]   Rohde & Schwarz, "Generation of Multi Carrier CW signals with SMU200A." Stockholm, 2003.

[29]   T. Broeck and J. Verspecht, "Calibrated Vectorial Nonlinear-Network Analyzers," presented at IEEE MTT-S, 1994, pp. 1069-72.

[30]   J. Verspecht, "Large-Signal Network Analysis," in *IEEE Microwave Magazine*, vol. 6, 2005, pp. 82-92.

[31]   W. V. Moer and Y. Rolain, "A Large-Signal Network Analyzer: Why is it needed?," *IEEE Microwave Magazine*, pp. 46-62, 2006.

[32]   D. Wisell, "A Baseband Time Domain Measurement System for Dynamic Characterisation of Power Amplifiers with High Dynamic Range over Large Bandwidth," Licentiate Thesis, Uppsala University, Uppsala, 2004.

[33]   J. Falk, "An electronic warfare perspective on time difference of arrival estimation subject to radio receiver imperfections," Licentiate Thesis, Royal Institute of Technology (KTH), Stockholm, 2004.

[34]   Rohde & Schwarz, "R&S SMU200A Vector Signal Generator, Specification ", 2007, http://www2.rohde-schwarz.com/.

[35]   Rohde & Schwarz, "Signal Analyzer R&S FSQ, Specifications," 2007, http://www2.rohde-schwarz.com/.

[36]   Y. Rolain and W. Moer, "Block-Oriented Instrument Software Design," *IEEE Trans. Instrum. Meas.*, vol. 53, pp. 830-38, 2004.

[37]   O. Andersen, N. Keskitalo, P. Stenvard, and D. Wisell, "Cost Effective High Performance Modular Instrumentation, Signal Generation and Signal Analysis for Future Mobile Communication Systems," presented at Autotestcon 2007, Baltimore, 2007.

[38]   http://www.ivifoundation.org/.

[39]   http://zone.ni.com/devzone/conceptd.nsf/webmain/ 7B38CE253B8D928C862571BE007BBF3C.

[40]   A. Moulthrop, C. Clark, C. Silva, and M. Muha, "A dynamic AMAM and AMPM Measurement Technique," presented at IEEE MTT-S, 1997, pp. 1455-58.

[41]   D. Wisell, M. Isaksson, and D. Rönnow, "Validation of Behavioural Power Amplifier Models Using Coherent Averaging," presented at Gigahertz 2005, Uppsala, 2005, pp. 318-21.

[42]   NTT Docomo, "NTT DoCoMo Achieves World's First 5Gbps Packet Transmission in 4G Field Experiment," 2007, http://www.nttdocomo.com/pr/2007/001319.html.

[43]   3GPP, "3GPP TS 36.211 3rd Generation Partnership Project; Technical Specification Group Radio Access Network; Physical Channels and Modulation, latest rev."

[44]   B. Johansson and T. Sundin, "LTE Test bed," *Ericsson Review*, pp. 9-13, 2007.

[45]   E. Dahlman, S. Parkvall, J. Sköld, and P. Beming, *3G Evolution: HSPA and LTE for Mobile Broadband*, Academic Press, 2007.

[46]   W. C. Black and D. A. Hodges, "Time Interleaved Converter Arrays," *IEEE Journal of Solid-State Circuits*, vol. 15, pp. 1022-29, 1980.

[47]   S. R. Velazquez, T. Q. Nguyen, and S. R. Broadstone, "Design of Hybrid Filter Banks for Analog/Digital Conversion," *IEEE Trans. Signal Processing*, vol. 46, pp. 956-967, 1998.

[48]   M. Seo, M. J. Rodwell, and U. Madhow, "Comprehensive Digital Correction of Mismatch Errors for a 400-MSamples/s 80-dB SFDR Time

Interleaved Analog-to-Digital Converter," *IEEE Trans. Microwave Theory Tech.*, vol. 53, pp. 1072-82, 2005.

[49]   Y.-M. Zhu, "Generalized Sampling Theorem," *IEEE Trans. Circuits and Syst.*, vol. 39, pp. 587-88, 1992.

[50]   P. Singerl and H. Koeppl, "Volterra Kernel Interpolation for System Modeling and Predistortion Purposes," presented at International Symposium on Signals, Circuits and Systems, 2005, pp. 251-54.

[51]   P. Singerl and H. Koeppl, "A Low-Rate Identification Method for Digital Predistorters Based on Volterra Kernel Interpolation " presented at 48th Midwest Symposium on Circuits and Systems, 2005, pp. 1533-36.

[52]   J. Tsimbinos, "Identification and Compensation of Nonlinear Distortion,", Doctoral Dissertation, University of South Australia, 1995.

[53]   T. Wang and T. J. Brazil, "Volterra-Mapping-Based Behavioral Modeling of Nonlinear Circuits and Systems for High Frequencies," *IEEE Trans. Microwave Theory Tech.*, vol. 51, pp. 1433-40, 2003.

[54]   A. Dienstfrey, P. Hale, D. Keenan, T. Clement, and D. Williams, "Minimum-Phase Calibration of Sampling Oscilloscopes," *IEEE Trans. Microwave Theory Tech.*, vol. 54, pp. 3197-3208, 2006.

[55]   L. Gommé, A. Barel, Y. Rolain, and F. Verbeyst, "Fine frequency grid phase calibration setup for the Large Signal Network Analyzer," presented at IEEE MTT-S, 2006, pp. 1444-47.

[56]   J. Pedro and N. Carvalho, "Designing Multisine Excitations for Nonlinear Model Testing," *IEEE Trans. Microwave Theory Tech.*, vol. 53, pp. 45-54, 2005.

[57]   D. Schreurs and K. Remley, "Use of Multisine Signals For Efficient Behavioural Modelling of RF Circuits with Short-Memory Effects," presented at ARFTG 61, 2003, pp. 65-72.

[58]   M. R. Schroeder, "Synthesis of Low Peak-factor Signals in Binary Sequences of Low Auto-correlation," *IEEE Trans. Inform. Theory*, vol. 16, pp. 85-89, 1970.

[59]   M. Solomou and D. Rees, "Crest Factor Minimization in the Frequency Domain," *IEEE Trans. Instrum. Meas.*, vol. 51, pp. 859-865, 2002.

[60]   M. Solomou and D. Rees, "Frequency Domain Analysis of Nonlinear Distortions on Linear Frequency Response Function Measurements," *IEEE Trans. Instrum. Meas.*, vol. 54, pp. 1313-1320, 2005.

[61]   P. Guillaume, J. Schoukens, R. Pintelon, and I. Kollár, "Crest-Factor Minimization Using Nonlinear Chebyshev Approximation Methods," *IEEE Trans. Instrum. Meas.*, vol. 40, pp. 982-988, 1991.

[62]   S. H. Han and J. H. Lee, "An Overview of Peak-to-Average Power Ratio Reduction Techniques for Multicarrier Transmission " *IEEE Wireless Communications*, pp. 56-65, 2005.

[63]   J. Tellado-Mourelo, "Peak to Average Power Reduction for Multicarrier Modulation," Doctoral Dissertation, Stanford University, 1999.

[64]   H. Ku and J. S. Kenney, "Behavioral Modeling of Nonlinear RF Power Amplifiers Considering Memory Effects," *IEEE Trans. Microwave Theory Tech.*, vol. 51, pp. 2495-2504, 2003.

[65]   D. Wisell, M. Isaksson, and N. Keskitalo, "A General Evaluation Criteria for Behavioral Power Amplifier Modeling," presented at ARFTG 69, Honolulu, 2007, pp. 251-55.

[66]   J. C. Pedro and S. A. Maas, "A Comparative Overview of Microwave and Wireless Power Amplifier Behavioral Modeling Approaches," *IEEE Trans. Microwave Theory Tech.*, vol. 53, pp. 1150-1163, 2005.

[67]   T. Liu, S. Boumaiza, and F. M. Ghannouchi, "Dynamic Behavioral Modeling of 3G Power Amplifiers Using Real-Valued Time Delay Neural Networks," *IEEE Trans. Microwave Theory Tech.*, vol. 52, pp. 1025-1033, 2004.

[68]   M. Schetzen, "Nonlinear System Modeling Based on the Wiener Theory," *Proceedings of the IEEE*, vol. 69, pp. 1557-1573, 1981.

[69]   M. Isaksson and D. Rönnow, "A Kautz-Volterra Behavioral Model for RF Power Amplifiers," presented at IEEE MTT-S, San Fransisco, CA, USA, 2006, pp. 485-88.

[70]   M. S. Heutmaker, E. Wu, and J. R. Welch, "Envelope Distortion Models with Memory Improve the Prediction of Spectral Regrowth for Some RF Amplifiers," presented at ARFTG 48, Clearwater, FL, USA, 1996, pp. 10-15.

[71]   J. Kim and K. Konstantinou, "Digital Predistortion of Wideband Signals Based on Power Amplifier Models with Memory," *Electron. Lett.*, vol. 37, pp. 1417-1418, 2001.

[72]   L. Rexberg, "Power Amplifier Predistortion," Patent WO 2004/086607, 2004.

[73]   M. Isaksson, D. Wisell, and D. Rönnow, "Nonlinear Behavioral Modeling of Power Amplifiers Using Radial-Basis Function Neural Networks," presented at IEEE MTT-S, Los Angeles, CA, USA, 2005, pp. 1967-70.

[74]   K. Remley, D. Schreurs, D. Williams, and J. Wood, "Extended NVNA Bandwidth for Long-Term Memory Measurements," presented at IEEE MTT-S, Forth Worth, TX, 2004, pp. 1739-42.

[75]   P. M. Asbeck, H. Kobayashi, M. Iwamoto, G. Hanington, S. Nam, and L. E. Larsson, "Augmented Behavioral Characterization for Modeling the Nonlinear Response of Power Amplifiers," presented at MTT-S, 2002, pp. 135-38.